STUDY OF EROSION WEAR OF PUMP MATERIAL FOR HANDLING WATER ASH SLURRY

Thesis submitted in partial fulfillment of the requirements for the award of degree of

Master of Engineering
In
PRODUCTION AND INDUSTRIAL

By:
Aseem Mishra
(Roll no. 800982001)

Under the supervision of

Mr. Satish Kumar
(Assistant. Professor, MED, Thapar University Patiala)

(July 2011)
Mechanical Engineering Department
Thapar University, Patiala-147004

CERTIFICATE

I hereby certify that the work which is being presented in the report entitled, "**STUDY OF EROSION WEAR OF PUMP MATERIAL FOR HANDLING WATER ASH SLURRY** ", in partial fulfilment of the requirements for the award of degree of Master of Engineering in Mechanical Engineering with specialization in **PRODUCTION AND INDUSTRIAL** submitted in **Mechanical Engineering Department** of Thapar University, Patiala, is an authentic record of my own work carried out under the supervision of **Mr. Satish Kumar** and refers other researcher's works which are duly listed in the reference section. The matter presented in this thesis has not been submitted for the award of any other degree of this or any other university.

15/07/11

Aseem Mishra

This is to certify that the above statement made by the candidate is correct and true to the best of my knowledge.

Satish Kumar
Assistant. Professor., MED
Thapar University
Patiala

Counter signed by

Dr. Ajay Batish
Professor & head
MED, Thapar University,Patiala

Dr. S.K. Mohapatra
Dean Of Academic Affairs
Thapar University, Patiala

ACKNOWLEDGEMENT

I wish to thank my thesis guide **Mr. Satish Kumar, Assistant Professor, MED, Thapar University** without whom, I would never been able to investigate about my work regarding this thesis. It is my proud privilege to express regards and sincere thanks to **Dr. Ajay Batish, Professor and Head, Mechanical Engineering Department, Thapar University, Patiala** for giving me the opportunity for the complete accomplishment of two years M.E. Course. I heartily thanks to Mr. Purshottam Kumar for his help in conducting the test on S.E.M. machine.

Finally, I would like to thank the entire faculty and staff of department of mechanical engineering, Thapar University, Patiala for helping me and giving me moral support by fulfilling my needs.

Aseem Mishra

ABSTRACT

Erosion wear is a serious problem that constantly accompanies the operation of the system for hydraulic transportation of solid materials. The consequences are the loss of material (steel); loss of work element's working capacity, great operational expenses, etc. The choice of new materials for working elements, improvements in construction, and optimization of the slurry flow are all various ways of softening the consequences of erosion wear that reflects on the working life of the hydraulic transportation pump's elements. The grey cast iron selected as a base material of pumping system. The electroplating technique is used for coating of nickel hard on base material. It is observed that the erosion wear of both coated and uncoated specimens shows inverse proportionality with impact angles being highest at 30º and lowest at 90º.Also the SEM images shows that the wear is mainly due to the scratching phenomenon due to brittle nature of grey cast iron specimens. The erosion wear increases with increase in flow velocities as at high velocities high kinetic energy is available at the surface of the specimen which causes more erosion wear to take place.

The erosion pot tester is designed for study of the erosion wear behavior of slurry transportation systems with high concentration.

TABLE OF CONTENTS

LIST OF FIGURES

LIST OF TABLES

CHAPTER 1

INTRODUCTION

Erosion wear is a serious problem that constantly accompanies the operation of the system for hydraulic transportation of solid materials. The consequences are the loss of material (steel), loss of work element's working capacity, great operational expenses, etc. The choice of new materials for working elements, improvements in construction, and optimization of the slurry flow are all various ways of softening the consequences of erosion wear that reflects on the working life of the hydraulic transportation pump's elements. *Wear can be defined as the continuous removal of material from the target surface*. This may occur due to various mechanisms namely corrosion, abrasion and erosion. Corrosion is the phenomenon of removal of material from the surface by chemical reactions due to unfavorable atmospheric conditions whereas abrasion and/or *erosion is defined as the mechanism of material removal from the target surface due impact of external agent on it*. In slurry transportation system, wear occurs mainly due to erosion. Erosion can further be classified into three categories as solid particle erosion, liquid impingement erosion and cavitation erosion. Solid particle erosion occurs due to direct impact of solid particles (present in slurry) on the pipelines, pumps and its components. Liquid impingement erosion is associated with the continuous impact of liquid jet on the target surface and cavitation erosion is defined as the repeated nucleation, growth, and violent collapse of cavities, or bubbles, in the liquid resulting in localized removal of material from the target surface. Researchers all over the world have been trying to reduce the wear through various techniques but it has been difficult to find out the common cause and remedy of this problem due to its variation and dependency on large number of parameters. The parameters that affect the erosion wear in slurry transportation systems are impact velocity, impact angle, size and shape of solid particle impacting on target surface, concentration of slurry, material of target surface, and particle size distribution in the slurry, slurry viscosity and combination of all of these.

Various techniques like field test, pilot loop plant test, coriolis tester and bench scale test have been carried out by researchers to experimentally evaluate the erosion wear for different target materials.

1.1 ASH DISPOSAL SYSTEMS

With the increase demand of electricity all over the world, industries and power plants have to boost up their production in order to satisfy the needs of people. Almost all coal fired thermal power plants are the major source for producing electricity in India. The coal burnt in these thermal power plants produces a large amount of ash as a residue (Figure 1.1). The ash produced may be of two types namely fly ash and bed or bottom ash. Around 100 million tons per year ash is produced at present. Out of this, around 80 million tons will be fly ash and the remainder will be bed ash.

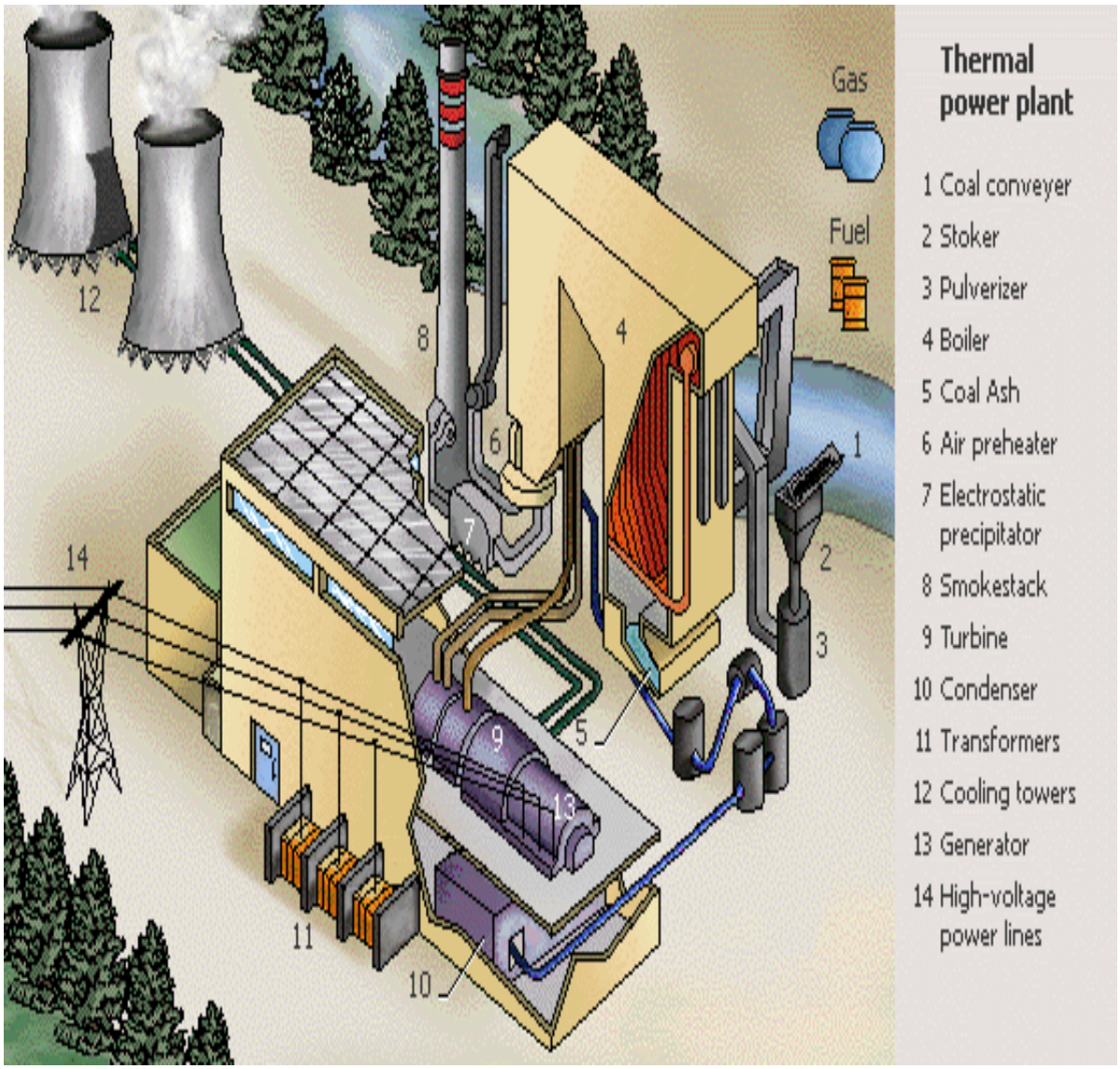

Figure 1.1 A view of thermal power plant

It has been investigated that fly ash is toxic in nature as it contains as main chemical components SiO_2 (51.4 wt %), Al_2O_3 (22.1 wt %) and Fe_2O_3 (17.2 wt%; ignited weight basis). As commonly observed, many toxic elements and heavy metals are highly enriched in the fly ash relative to the original coal. For example, considerable amounts of Be (16.4 ppm), Cu (106 ppm), Zn (578 ppm), As (40.4 ppm), Cd (2.6 ppm), Hg (18 ppm), Pb (71 ppm), and U (21.8 ppm) is found in Fly ash. Hence it is necessary for the safe disposal of ash (fly and bottom both) away from the power plants and society. Hence to achieve this objective various thermal power plants employ ash handling systems. Ash is transported in the form of slurry (prepared by mixing ash with water in definite proportions) from thermal power plants to ash ponds. This slurry is transported or disposed through pipelines, pumps, impellers etc. employed in ash handling systems (Figure 1.2).

Figure 1.2 Ash slurry disposal systems

From the past few years it has been found out by many researchers that by the time of operation of slurry transportation systems, there occurs wear in various parts of systems such pipelines, pumps and its components impeller turbine etc (figure 1.3) . The operation of ash disposal pipelines is highly uneconomical due to requirement of large quantity of water and increase in power consumption for pumping 80-90% of clear water. Further, bed ash is relatively coarse as compared to fly ash which is extremely fine. The transportation of the mixture of both the ashes at low concentration also require higher flow velocities and result in existence of highly skewed concentration profile across the pipe cross-section. This causes excessive erosion wear of the components of ash disposal system and therefore reduces their working life.

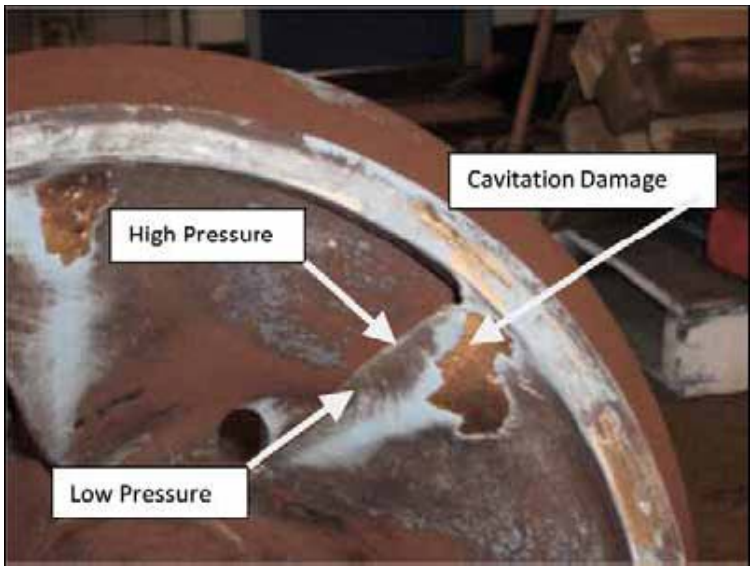

Figure 1.3 Slurry erosion in pump casing

1.2 WEAR

Wear is defined as progressive volume loss of material from a solid surface due to corrosion, abrasion and erosion. Wear is one of the most common problems encountered in industrial applications. It is defined as the erosion of material from a solid surface by the action of another solid. In the domain of wear, particularly the wear encountered in handling abrasive solid particles, much work has been done in the past half century with regard to dry" abrasivity, but only in more recent years has interest grown in 'wet' abrasivity, namely slurries. Wear can be classified into following types.

1.2.1 Adhesive wear

Adhesive wear is the only universal form of wear; it arises from the fact that, during sliding, regions of adhesive bonding, called junctions, form between the sliding surfaces. If one of these junctions does not break along its original interface, then a chunk from one of the sliding surfaces will have been transferred to the other surface. In this way, an adhesive wear particle will have been formed. Initially adhering to the other surface, adhesive particles soon become loose and can disappear from the sliding system. One of the significant things about adhesive wear is that at the interface, or the point where it touches another metal surface, it must be very hot in order for the micro welding to take place at all. That is what adhesive wear is — microscopic welding. The heat produced at the contact interface is very high — near the melting point of the two metals touching each other. This heat mostly comes from the stress of contact and not from the temperature of the environment.

1.2.2 Abrasive wear

Abrasive wear is produced by a hard, sharp surface sliding against a softer one and digging out a groove. The abrasive agent may be one of the surfaces or it may be a third component (such as sand particles) Abrasive wear coefficients are large compared to adhesive ones. Thus, the introduction of abrasive particles into a sliding system can greatly increase the wear rate; automobiles, for example, have air and oil filters to catch abrasive particles before they can produce damage. On the abrasive specimen, the surface shows a scratched appearance from hard particles digging into it as they were moved across the surface.

1.2.3 Corrosive wear

Corrosive wear arises when a sliding surface is in a corrosive environment, and the sliding action continuously removes the protective corrosion layer, thus exposing fresh surface to further corrosive attack. Corrosive wear occurs as a result of chemical reaction on a wearing surface. The most common type of corrosion is mainly due to 13 reactions between metal and oxygen. These oxides are wiped away with the flow and cause pitting of the surfaces. Corrosion is accelerated as impacted surfaces are exposed to slurry chemistry.

1.2.4 Surface fatigue wear

Surface fatigue is a process by which the surface of a material is weakened by cyclic loading, which is one type of general material fatigue. Surface fatigue wear occurs as result of the formation and growth of cracks. It is the main form of wear of rolling devices such as ball bearings, wheels on rails, and gears. During continued rolling, a crack forms at or just below the surface and gradually grows until a large particle is lifted right out of the surface.

1.2.5 Erosive wear

Erosion wear is the dominant process and can be defined as the removal of material from a solid surface due to mechanical interaction between the surface and the impinging particles in a liquid stream. Erosion involves the transfer of kinetic energy to the surface. This means that in erosion material removal is a function of particle velocity squared to higher power.

1.3 PARAMETERS AFFECTING EROSION WEAR

The parameters that affect erosion wear are as follows:

1.3.1 Impact angle

It is defined as the angle between the target surface and the direction of the impact velocity of the solid particle impinging on that surface. The variation of erosion wear with the impact angle depends on the characteristics of the target surface material namely brittle or ductile type.

1.3.2 Impact velocity

It is defined as the linear velocity of the solid particle striking on the target surface. The erosion rate is generally related to the particle velocity using power law relationship in which the power index for velocity varies in the range of 2-4.

1.3.3 Concentration of slurry

Concentration is the amount of solid particles by weight suspended in a fluid. Erosion rate increases with increase in concentration of particle size because due to high concentration, more solid particle will tend to strike on the target surface resulting in the erosion to take place.

1.3.4 Particle shape and size

The shape of the solid particle is also a dominant factor affecting the erosion wear. For sharp edged solid particle erosion wear will be more due to deep indentation. The erosion wear also increases due to increase in particle size according to the power law relationship.

1.3.5 Hardness

Hardness is the characteristic of a solid material expressing its resistance to permanent deformation. Erosion wear depends on the hardness ratio which is defined as the ratio of hardness of the target material to the hardness of the solid particle.

1.4 DIFFERENT TYPES OF TEST RIGS

It is essential to have some information on erosion wear at design stage so as to predict the service life of component and adopt preventive maintenance, if any. The mechanism of material removal due to solid-liquid mixture varies with the field condition and therefore, different types of bench scale test rigs were developed to simulate these conditions. The different bench scale test rigs used so far are discussed in this section with their basic working principle.

1.4.1 Miller Test Apparatus

This test apparatus is designed and developed by Miller [1974] to evaluate relative abrasion wear of different materials and is shown schematically in Figure 1.4. ASTM has accepted this test method for evaluating slurry abrasivity (Miller Number) and slurry abrasion response of material (SAR Number). The test data obtained by this method is used to determine a Miller Number, which is applied for estimating the service life of pipe, pumps, valves etc[b]. In this test method, the wear test specimen is fixed in a sample holder attached to a reciprocating arm carrying a load of 22.24 N, which run in a standard sand slurry. The wear sample of size 25.4 mm x 12.7 mm is to be tested for around six hours and its weight loss is measured in the interval of each two hours. The data obtained from this test method are used to compare the relative erosion behaviour of the two materials and thus the Miller test can be used for selection of pipe material for given slurry. Another version of Miller test apparatus was developed by Roco et al**.** (1987), which is known as sliding bed apparatus.

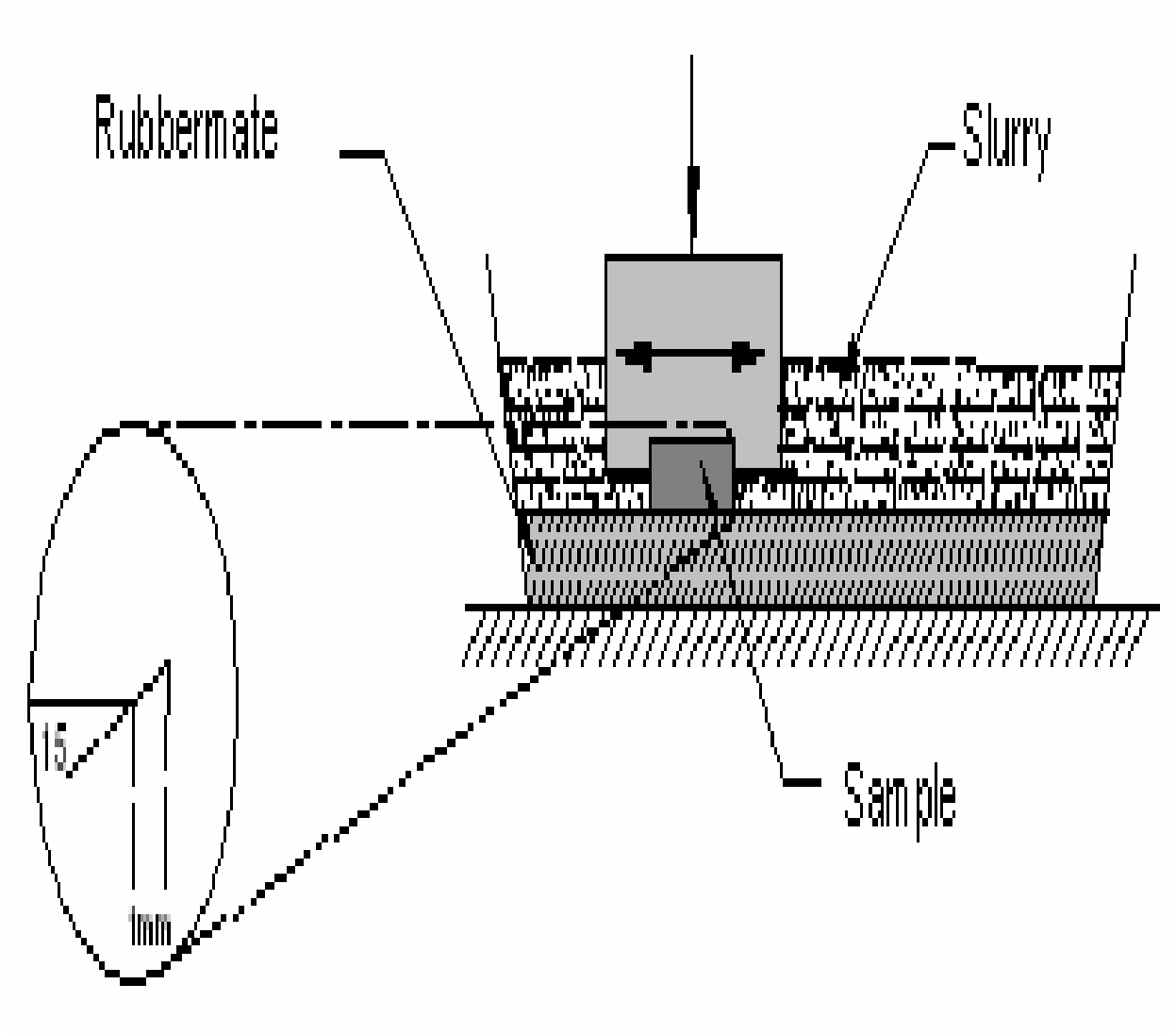

Figure 1.4 Miller test apparatus

This is primarily used to simulate slurry erosion wear due to friction as observed in sliding bed 13 flow. In this test apparatus, the wear specimens were fixed at the bottom of a close end horizontal pipe piece, which is filled with the solid-liquid mixture and reciprocated with known velocity. The mass loss of the wear specimen is used to evaluate the wear rate.

1.4.2 Jet Impingement Tester (JIT)

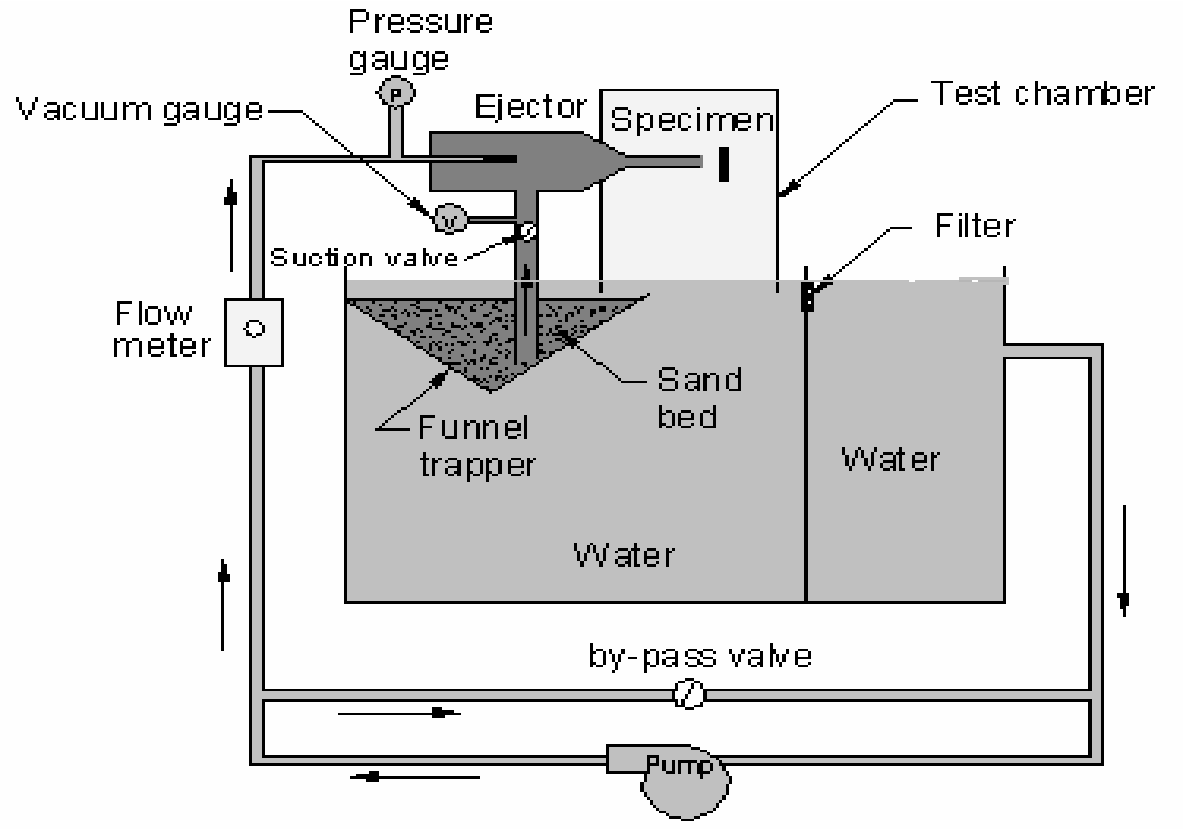

Figure 1.5 Jet Impingement Test Rig

In this type of test rig, a flat specimen is subjected to a jet of solid-liquid mixture as shown in Figure 1.5**.** The specimen can be oriented at different impact angles in the range of 0 to 90°. It comprises of a pump and an ejector to issue a jet through a nozzle. Jet impingement tester simulates the wear for direct impact of solid particles in equipments such as pumps, bends, tee junctions, elbows, contractions etc.

1.4.3 Concentric Cylindrical Test Rig

Concentric cylinder viscometer was used by Shook and Pilling [1987] to simulate pipe wall erosion. The outer cylinder is rotated and the inner cylinder is kept stationary[b]. A small radial clearance of around 5-6 mm was maintained between the two cylinders and the weight loss of outer cylinder is used to evaluate the erosion wear. This device can be used when the difference in density of liquid and solid particles is less as the particles may settle during the wear test.

1.4.4 Coriolis Erosion Tester

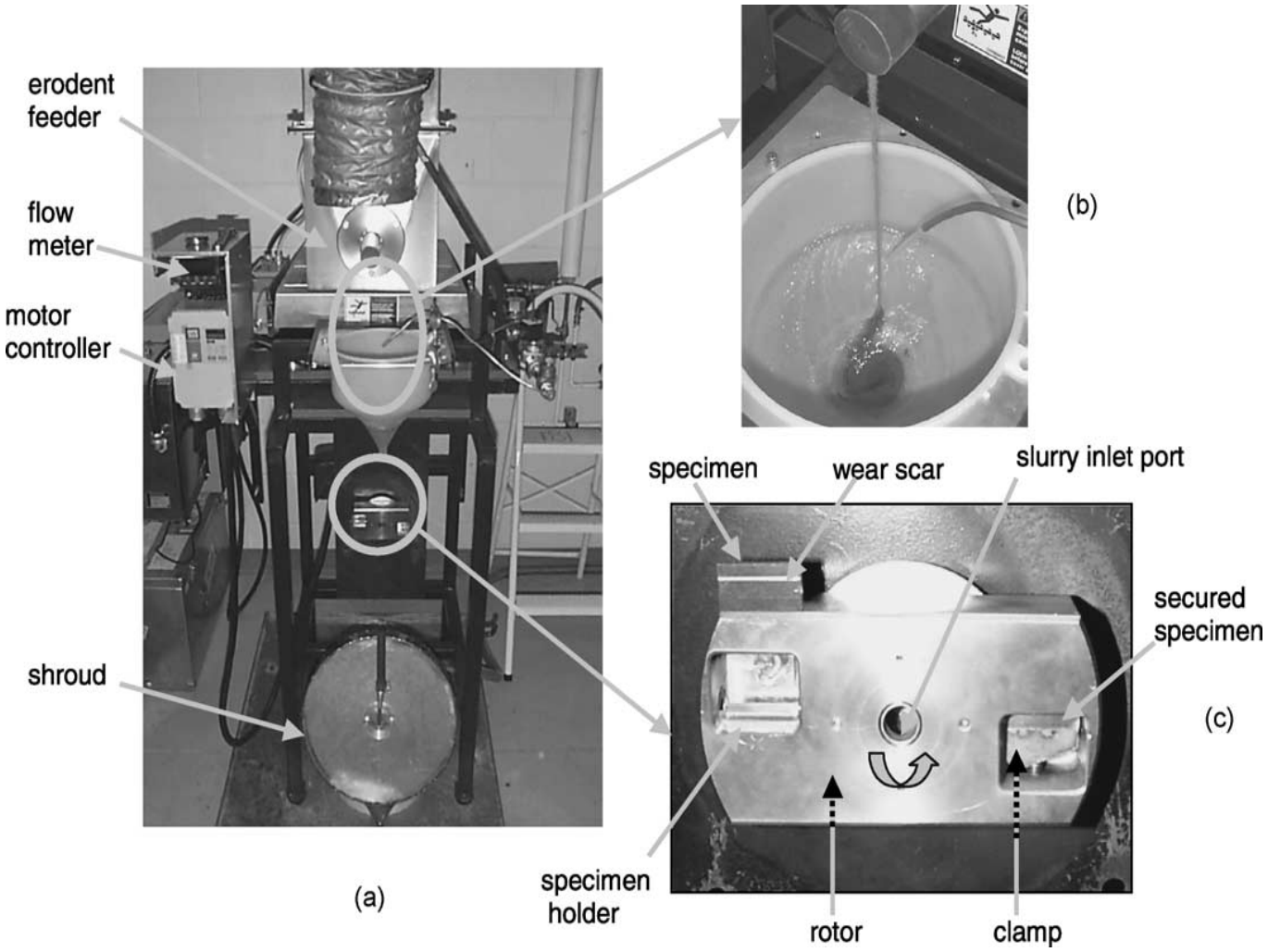

Figure 1.6 Coriolis erosion test rig

Coriolis slurry erosion tester was first developed by Tuzson [1984] to simulate the conditions obtained in slurry pump, pipeline and cyclones. In this test rig, the slurry is accelerated centrifugally from a rotating bowl through two small radial channels located at 180º apart. The wear specimens are to be fixed on the channels. The Coriolis force increases the slurry interaction with the back wall of the wear specimens. Clark et al. [2000] modified this tester, as shown in Figure 1.6, with an arrangement to mount flat specimen on either side of a diametric slot in a solid rotor.

This test rig consists of a150 mm diameter rotor containing a diametric passage of 12.7 mm bore. The flat plate specimen holders are located on either side of then diametric passage at

equidistant from the rotation center. The specimen holders comprises of a passage of 1 mm wide and 6.35 mm high. The wear specimens are attached at the bottom of the specimen holder which is flat rectangular blocks with approximate dimensions of 29 mm x 15 mm x 6 mm. Slurry, from the central chamber is constrained to flow outwards through the channel. As the rotor is turned, the erodent particles are directed to the wear specimen surface due to the Coriolis force.

1.4.5 Centrifugal Erosion Tester

Centrifugal erosion tester can be used in either vacuum or atmosphere conditions. The erodent particulate slurry is fed into the center of a rotor by means of conical vessel as shown in figure to move outwards along radial channels as shown in Figure 1.7 .The slurry leaves the rotor at a speed governed by the peripheral speed of the rotor [Soderberg et al. (1981)]. Stationary specimens are arranged around the rim of the rotor, and the method can be used to compare the erosion behaviour of different materials. This type of erosion tester has also been modified and used by Hayashi et al. [2005] to evaluate the erosion rate of different materials at elevated temperature.

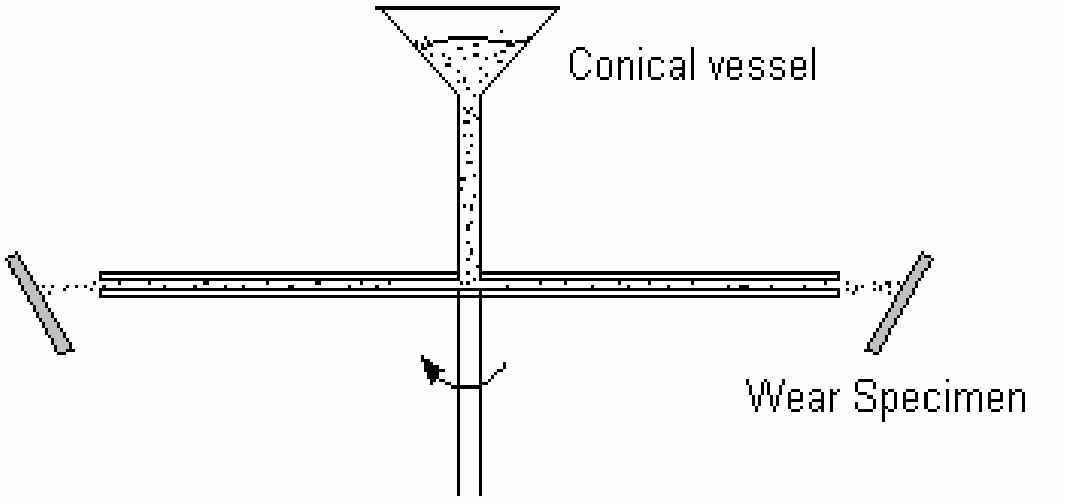

Figure 1.7 Centrifugal erosion tester

1.4.6 Falling Jet Test Apparatus

In falling jet test apparatus, the wear specimens were rotated in a vacuum chamber and a jet of solid-liquid mixture falls on the specimen due to gravity flow. This test apparatus was designed and developed by Lin and Shao [1991A] to study the effect of particle impact angle. In this test

rig, four wear specimens of size 25 mm x 10 mm x 5 mm were clamped in specimen fixtures mounted on four horizontal arms rotated by a variable speed electric motor. The radius of each arm was 104.5 mm. This assembly is kept in a vacuum chamber as shown in Figure 1.8[b]. The slurry in the chamber falls freely under gravity from a barrel of 25 liters capacity where a stirrer is used to keep the solid-liquid mixture under suspension. The impact angle and velocity are calculated from the vector addition of the fall velocity and rotating speed of the specimens. The partial vacuum in the chamber of the specimens minimizes the spreading effect of jet, which generally occurs in jet impingement tester. However, difficulty in maintaining the partial vacuum in the chamber limits the use of this test rig.

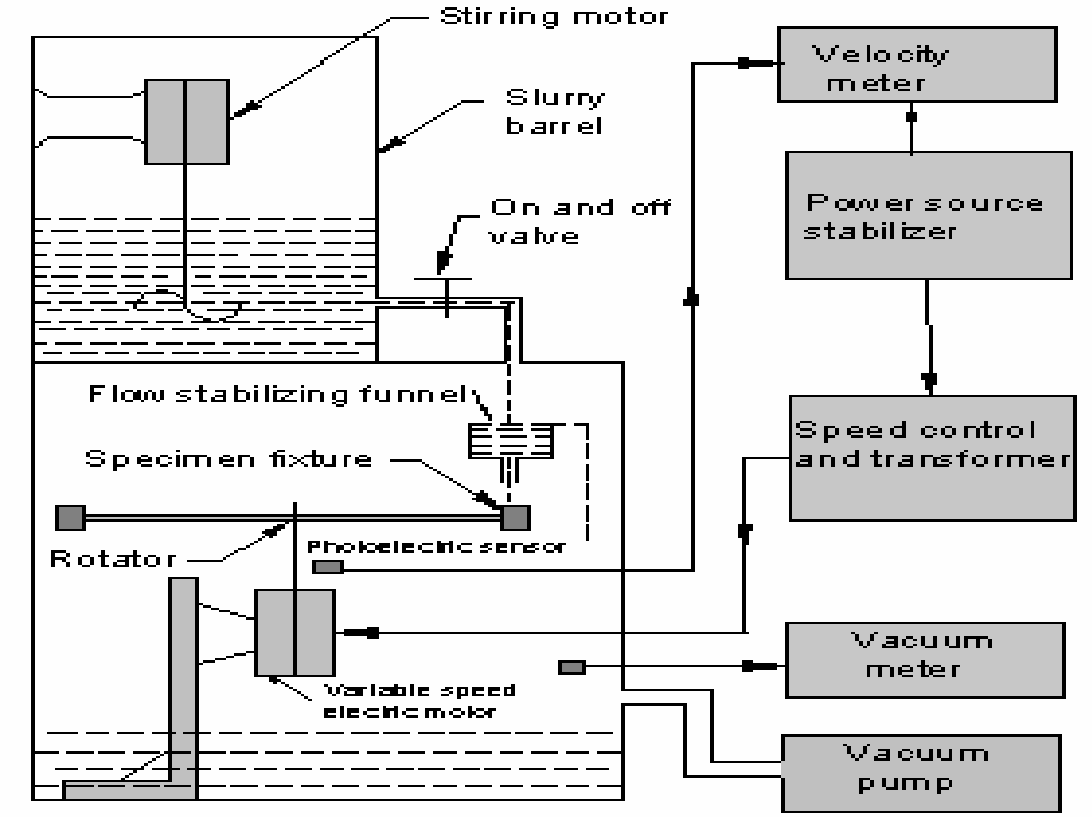

Figure 1.8 Falling jet test apparatus

1.4.7 Jet-in-slit Apparatus

Zhao et al. [1999] and Yabuki et al. [2000] have used this test rig to investigate the slurry erosion properties of different types of coatings. This test rig contains a transparent tank consisting of

two compartments; a lower one which is smaller in diameter to store concentrated mixture and an upper one of bigger diameter to store liquid only as shown in Fig. 1.9.

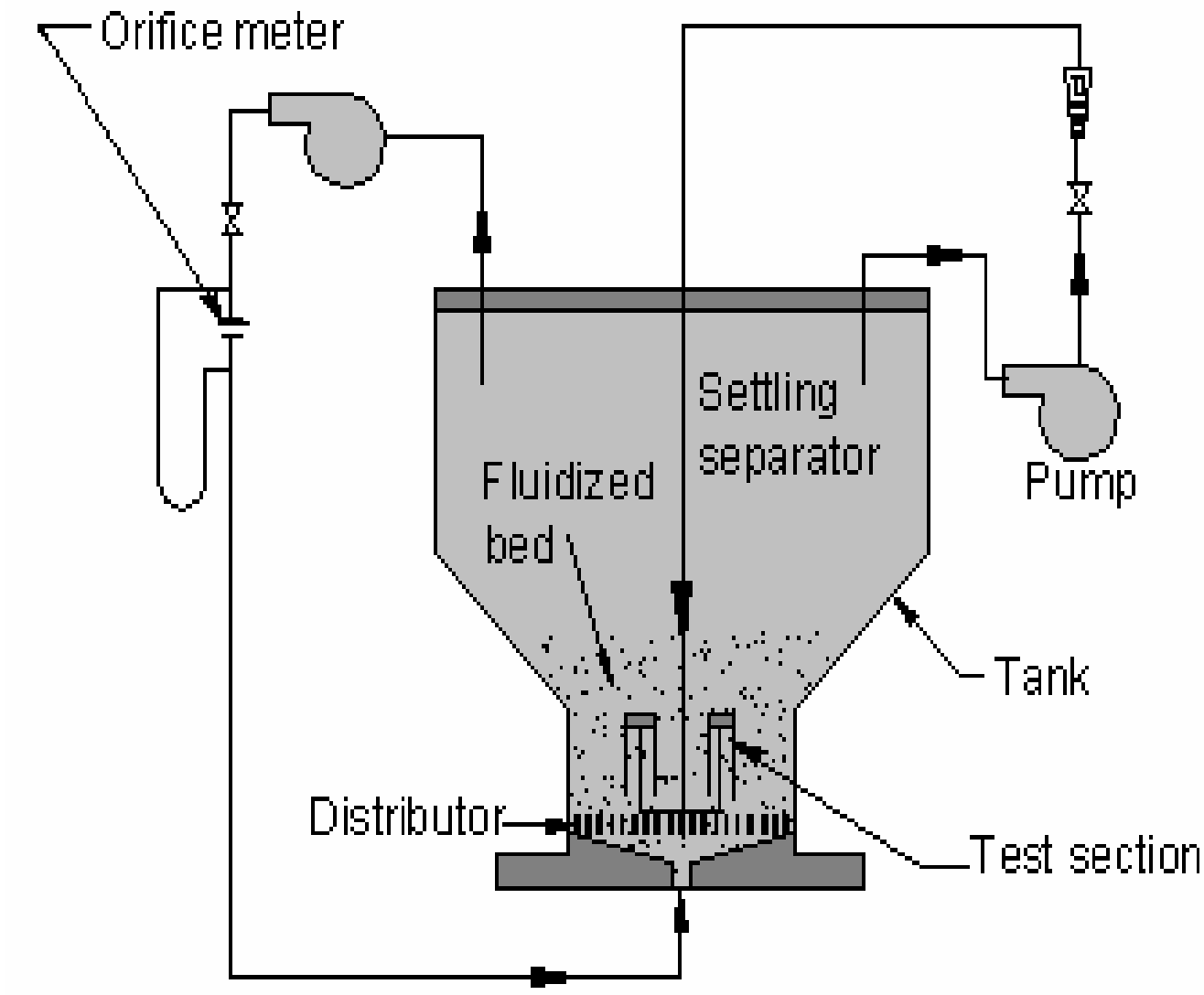

Figure 1.9 Jet in slit apparatus

The upper tank contains clear water which is circulated by the pump into the test section containing four test specimens subjected to uniform upward flow and remaining water is utilized to set up the fluidized bed in lower tank.

The liquid jet from the nozzle, located at the center of the test section, sucks up the slurry, which is mixed with the jet fluid to impinge on the test specimen, and thereafter, the mixture is radially exhausted through the slit between the specimen and the guide plate. The concentration of solid particles in the fluidized bed can be easily regulated, by controlling the flow rate of the liquid fed to the distributor.

CHAPTER 2

LITERATURE SURVEY

Ahmed Elkholy et al [1] (1983) conducted experiment on aluminium and cast iron having Brinell hardness 121 and 230 respectively. He used the equation, $W = KV^n$. W is wear in term of mass loss of specimen per gram of sand and K is constant corresponding to other parameter like concentration of slurry, particle size and impact angle. The value of n is determined by value of different velocities fitting in above equation. Then Belzona molecular ceramic steel (BMS) was tested under identical condition as for Al and Cast Iron. The observation showed that wear increase with increase in velocity.

M. A. Rayan & M. Shawky [2](1989) studied the erosion of a cast steel impeller at two flow velocities 0.64 m/s and 0.85 m/s at concentration 2% and 4% (by volume) of sand slurry. They concluded that weight loss rate (WLR) is proportional flow velocity. They suggested the following relation

$$\text{Wear } \alpha \text{ Flow velocity}^n \quad \text{.....} \quad (2.1)$$

The value of exponent n is approximately equal to 3.

Gupta [3] (1995) observed significant variation in wear from the top to bottom of the pipe (i.e. uneven wear at the cross section of pipe) and attributed this phenomenon to skewed distribution of concentration profile and particle size across the pipe cross section. He related the wear at any location of the pipeline with the local values of concentration and particle size.

Clark[4] (1995) conducted experiments on electro-polished OFHC copper using 540 μm size glass particles in diesel oil and air. He found that the impact craters formed during slurry erosion were smaller than those formed during gas-solid erosion at the same nominal test speed. Thus the material removal rate due to the solid particles suspended in gas or air is higher than the particles suspended in liquid. However, the mechanisms of material removal were observed similar for gas or liquid media. The difference in the wear rates has been attributed to liquid properties namely, density, viscosity, boundary lubrication, lubricity, squeeze film, cushioning effect, pH value, etc.

Mishra [5] et al. (1998) conducted experiments in a pilot plant loop to investigate the wear behaviour of three designs of bend, namely two diverging converging and one conventional. They observed that diverging-converging bend shows less wear, which was been attributed to development of secondary flow. They proposed the improvement in the bend design for reducing the wear

Gandhi and Shesadri [6] (1999), has conducted the experiments on rectangular brass wear pieces (hardness=RC45, specific gravity=8.5) in a pot tester arrangement assuming the parallel flow wear i.e. the direction of impact velocity is parallel to the plane of wear surface. The range of the velocity was 3m/s to 9 m/s and three narrow size particulate slurries (890µm, 448.5µm and 223.5µm) were taken. The concentration of slurry was ranging from 20%-40%. In their results they found that wear increases linearly with increase in velocity and the slope of line increases by increasing any other parameter such as concentration and particle size. Based on the results, he established the relationship as follows:

$$E_w = 2.57V^{2.56}C_w^{0.83}d^{0.85} \quad \text{.....(2.2)}$$

Where E_w= wear, V= velocity, C_w= Concentration, d= particle dia.

They concluded that parallel flow wear largely depends on the velocity as compared to solid concentration and particle size.

Stack and Pungwiwat[7] (1999) reported that erosion rate does not increase continuously with increase in the particle size. According to them, the variation of wear with particle size is also influenced by particle shape and impact velocity. They attributed this phenomenon to the fluid dynamic effects i.e. complex behaviour of suspension of particles of different sizes, in the test rig used. The large variation in the exponent value of particle size has also attributed to variation in its shape. Natural erodents consist of particles of different shapes, even for the same size group.

Sellgren et al [8] (2000) showed that the addition of clay to sand slurries has been found to reduce the pipeline friction losses, thus lowering the pumping head and power consumption. Pump water heads and efficiencies are decreased by the presence of solid particles. Experimentally results are presented for a centrifugal pump with an impeller diameter of 0.625 m for three narrowly graded sands with average particle sizes of 0.64, 1.27 and 2.2 mm. Reductions

in head and efficiency are lowered by about one third for sand clay mixtures with sand to clay mass ratios between 4:1 and 6:1.

Craig I. Walker and Greg C. Bodkin [9] (2000) observed that effect of particle size onside liner material (cast iron) wear was not significant for STD impeller. They also observed that wear rate for particle size 150µm, 500µm, 1000µm was nearly same. But for HE assembly it was the dominant variable. The wear rate is proportional to particle size.

Gandhi et al [10](2001) observed that weight loss of a brass specimen increase with increase in volute angle and attained a maximum value at 178º angle with flow rate 18 lps. Slurry used is Zinc tailings material at 20% and 30% concentrations. For volute angle between 180º to 300º, the wear is smaller. He pointed out that the impact angle of solid particles decrease with increase in volute angle around 90º at tongue and nearly zero at nozzle. The wear along casing is the function of variation of impact angles of solid particles along the casing.

C.I.Walker et al [11] (2001) compared the wear rate result of lab test and field test on side liner of STD and HE configurations of impellers. He found that the lab wear rate with cast iron material was greater than the wear rate for the field results with the white cast iron due to different hardness of parts. Both materials showed excellent similarities in wear rate trend with particle size. It is found from field result that \rubber show lower wear rate than the metal for equivalent particle size < 700µm. This was because the rubber surface can absorb smaller particle impact energy without significant cutting tearing.

O. Flynn et al [12] (2001) developed an analytical model for predicting the wear rate based on the toughness and strain energy of the target material. The model 24 is used to predict the erosion rate of heat-treated steels at different impact angles, which showed reasonable agreement with experimental measurements. They reported that the erosion resistance increases with increase in the value of the product of toughness and strain energy of the target material

S.N. Singh and Gandhi [13] (2003) has conducted experiments in a pot tester for analysing the effect of orientation of plane surface relative to its motion in solid-liquid suspensions. They conducted experiments at various operating conditions by varying the impact angle, defined as

the angle between the tangent to the plane surface and its velocity. Flat brass test pieces flush with a surface of hardened carbon steel plate (hardness= RC45) were taken. The orientation or impact angle was varied from 0° to 90° and concentration range was 20-40%. It has been found out that the erosion wear decreases with increase in orientation angle but this decrease was not consistent. It was seen that wear increases with the increase in orientation angle till 30° and then decreases with increase in orientation angle up to 90° for various range of velocities and particle sizes. Further it has been concluded that wear at 30° angle was 3-4.5 times higher than at 90° orientation angle and also wear increases with increase in velocity and particle size but decreases with increase in solid concentration under different impact angles.

R.J. Llewellyn et al[14](2004) has performed coriolis test for assessing the scouring attack resistance of some cast alloys used for slurry pump components. The materials involved range from high toughness nickel chrome molybdenum steel; corrosion resistant stainless steels; comparatively low carbon irons with high chromium contents which provide corrosion and some wear resistance and finally to higher carbon and chromium variants which have extremely high erosion and abrasion resistance properties. They reported that the erosion resistance increased with hardness, with higher nominal carbon content and carbide volume fractions and with decreasing carbide size. Further Hypereutectic chrome white irons exhibited high Coriolis erosion resistance.

Gandhi and Borse [15] (2004) had conducted experiments to determine the nominal size of multi-sized slurry representing the erosion wear and the effect of presence of fine particles (< 75µm) in the slurry. Wear specimens of grey cast iron were taken. The range of orientation angle was 0° to 90°. The slurry was prepared of water with sand collected from the banks of river Narmada. Overall specific gravity of sand was 2.68 and the final static settled concentration was observed as 53.7%. Mean particle size of slurry was taken as 505µm. The range for narrow size particulate slurry was 112.5µm to 855µm and multi sized slurry was prepared by mixing equal amount of different narrow sized slurries. Based on the results of their experiments they concluded that for narrow size slurry mean particle size can be taken as the effective particle size whereas for multi sized slurries, weighted mass particle size seems to be better. It has also been

concluded that effect of finer particles in both narrow and multi sized slurries reduces the erosion wear.

Aubin et al.[16] (2004) have used a particle image velocimetry (PIV) system to analyze the flow field due to rotation of a pitched blade turbine (PBT) propeller in a cylindrical pot using liquid only. They observed different flow patterns for down-pumping and up-pumping modes of rotation of the propeller. The flow pattern for down-pumping mode depicted a single circulation loop near the propeller extending around three-quarters of the tank. The liquid velocities are low near the top surface of the tank due to poor circulation. Whereas for up-pumping mode, two distinct circulation loops, one in the lower part and another in the upper part of the tank were observed. In up-pumping mode, the liquid is drawn from the lower side of the tank and forced to flow upwards at an inclination equal to the blade angle, which generates more random motion in the upper part of tank.

Desale et al [17] (2005) has made an attempt to improve the design of a pot tester by minimizing the effect of propeller rotation while ensuring the uniform distribution of solids. Initially experiments were conducted in a transparent cylindrical tank with PTB propeller to determine the optimum speed required for uniform distribution of solids. Flat wear test specimens are then rotated in the cylinder at different speeds opposite to the rotational direction of the propeller while keeping the speed of the later constant. The wear specimens were oriented at different angles with respect to the rotational direction and care was taken to minimize its effect on suspension of solids in the pot. Experiments on erosion of aluminium alloy AA6063 in sand–water mixture has been carried out to find suitability of the device for wear evaluation. When the propeller was rotated in down pumping mode it was observed that the motion of particles was obstructed by baffles. Hence same propeller was then rotated in down-pumping mode and this phenomenon was almost disappeared except slightly higher concentrations near the baffles due to swirling motion produced by the propeller. While the propeller is rotating, he observed that there exists a minimum propeller speed at which the mixture appeared to be uniformly distributed. The speed was called as suspension speed. The suspension speed was found to be around 305 rpm and the specimens were rotated at 404rpm in the opposite direction to that of propeller to achieve the minimum peripheral velocity of 3m/sec. Finally it has been concluded that the design of pot tester is intended to conduct wear tests at moderate solid concentrations

and actual flow velocities to simulate the wear conditions for pipeline, bend, pump etc. and may provide more realistic results.

S. Das et al [18] (2006) studied the erosion-corrosion wear of aluminium alloy composites. The LM13 alloy and LM13-Sic composites were taken to study the effect of sand concentration on the wear behavior in acidic and marine environment for a traversed distance of 763km and a rotational speed of 900rpm. They observed that the wear rate increase with increasing sand concentration irrespective of the material. This is because as the concentration of sand in the slurry increases the severity of erosion /abrasive attack increase because a greater number of particles are impinging on the surface. On the other hand, the slurry of corrosion attack may decrease because the effective volume of the corodent decreases. The alloy exhibited higher wear rate compared to the composite as sand concentration increased from 0% to 40%. It was concluded that all the material exhibited higher wear rate in the acidic media as compared to NaCl at 0% and 20%sand concentration. However at 30% and 40% sand concentrations the material posses lower wear rates in acidic media.

G.R. Desale et al[19](2006) conducted an experiment to show the variation of erosion rate with orientation angle for solid liquid mixture of three natural erodent (quarts ,alumina ,and silicon carbide) for ductile target material AA 6063 and A1513042 steels the test performed in a pot tester rotating specimen at 3 m/s in 10wt% concentrated slurry having particle size 550µm.They pointed out that as the orientation angle increases the erosion rate first increase up to a maximum and then decreases to a steady state till 90º. Both the target material show maximum wear at shallow angles with all three erodents. The max wear angle was observed as 15º and 22.5º for AA6063 and AISI 304L steel respectively. Further it has been concluded that angle for maximum wear is a function of target material properties and does not depends on erodent properties.

T. Manisekaran and M. Kamaraj[20] (2006) had studied the effect of particle size and impingement on surface modified 13Cr-4Ni stainless steels (as they are generally used for hydro turbines and water pumps). Samples of dimension of 50×50 mm^2 were machined from 6 mm thick cast 13Cr-4Ni steel plates and the surface modifications were done by two methods namely laser hardening and pulsed-plasma nitriding. Tests were carried out in a test rig to study the erosion performance of modified layers with two different erodent Particle size ranges (less than

150 and 150-300 lm) in a silica sand slurry for 2 h at 90°. After surface modification they observed that pulsed plasma hardened steels showed more hardness than laser hardened steels but based on their experiments they found interesting results that laser hardening of 13Cr-4Ni steels exhibited better erosion resistance at all angles of impingement than pulse plasma nitriding. This may be attributed to martensitic transformability of the retained austenite coupled with moderate hardness in laser hardened steels. Pulsed-plasma nitrided steels could not withstand repetitive stresses arising out of jet impingement and, underwent chip formation and micro cutting. It had also been concluded that the amount of erosion with erodent size range 150-300μm was two times more than the amount of erosion with erodent size range less than 150 μm and SEM examination clearly revealed that plastic-deformation mode was primarily responsible for material removal in laser-hardened steels.

M.C. Lin et al [21] (2006) conduct experiment to study high-speed slurry erosion characteristics on the test specimens of NiCrBSi coating prepared by using the high velocity oxy-fuel spraying technique with a post-thermal treatment. The composition of powder used for spraying is Ni–17Cr–3B–4Si–4Fe–1C (wt.%). The sprayed coating had a 1.5 mm thickness and exhibited a melting temperature of 1050 °C. The substrate used was AISI 1045 carbon steel. Sand water mixture with particle size of 263-363μm is used as impingement medium. SUS304 stainless steel was selected as the comparison material. Experimental results show that the NiCrBSi sprayed coating exhibits a much better slurry erosion resistance than the SUS304 stainless steel because of he post-thermal-treated NiCrBSi coatings have an extra high hardness and small quantity of porosity. A preliminary test has revealed that the NiCrBSi spray coating can increase significantly the using-life, 3–4 times, of needles and nozzles in hydraulic machinery. The erosion rate for the NiCrBSi sprayed coating slightly increases with the impinged angle. However, a maximum erosion rate appears at an impinged angle of around 30° for SUS304 stainless steel. Both NiCrBSi sprayed coating and SUS304 stainless steel exhibit impinged surfaces with lots of furrows at an impinged angle of 30°. At a high impinged angle of 90°, the SUS304 stainless steel exhibits an impinged surface with lots of overlapping and irregular concavities, while, these features are less obvious for NiCrBSi sprayed coating. The hardness of SUS304 stainless steel increases significantly with increasing impinged angle during the high-speed slurry erosion.

But, there is no obvious work hardening for the NiCrBSi sprayed coating due to its extra-high hardness and less plastic deformation, even at a high impinged angle of 90°. The surface morphologies exhibit lots of long furrows and ridges at a low impinged angle of 30°, regardless of the SUS304 stainless steel or NiCrBSi sprayed coating. At a high impinged angle of 90°, the SUS304 stainless steel exhibits an impinged surface with lots of overlapping and irregular concavities due to the deformation of microforging and extrusion. However, these features are less obvious for NiCrBSi sprayed coating, due to its extra-high hardness and the micro-porosities existing within the sprayed coating.

S.M. Ahmed et al[22] (2007) has investigated about the influence of impingement angle on erosion mechanisms of 1017 steel and high-Cr white cast iron using a slurry whirling-arm test rig. In their results it was found that showed that, the effect of impingement angle on erosion mechanisms of 1017 steel has three regions. In the first region ($\theta \leq 15°$) shallow ploughing and particle rolling were the dominant erosion mechanisms, micro cutting and deep ploughing in the second region ($15° < \theta < 75°$), while indentations and material extrusion prevailed in the third region ($\theta \geq 75°$). For high-Cr white cast iron the test results showed that, the erosion mechanisms involved both plastic deformation of the ductile matrix and brittle fracture of the carbides. At low impingement angles (up to 45°) observations of microphotographs of the impacted surfaces revealed that, plastic deformation of the ductile matrix was the dominant erosion mechanism and the carbides fracture was negligible which lead to small erosion rate. Whereas, at high impingement angles (greater than 45°) gross fracture and cracking of the carbides were the main erosion mechanisms in addition to indentation with extruded lips of the ductile matrix.

M.N. Noui-Mehidi et al[23] (2007) has experimented the effect of paint layers on stainless steel specimen in a slurry-mixing tank in which 10 painted samples mounted on a shaft were rotated at constant speed for a certain interval of time. The slurry was a mixture of tap water and alumina particles with a concentration of 15% (v/v). Different type of paints such as Gloss Enamel paint, Epoxy Enamel, Standocryl 527 two-pack paint etc were applied on steel specimen by spray guns operated with compressed air. The effect of impact angle on the particular type of paint was investigated by orientating the samples consecutively at angles from 0◦ to 90◦ with an increment of 10◦. They found that in the slurry medium, most soft paints, such as “Enamel” type have

similar erosion maps to ductile materials with a maximum wear rate at around 30°. Metallic paints and styrene type paints have shown a slightly higher angle of 40◦ for maximum erosion.

Feng Jianjun et al[24] (2007) have conducted numerical simulations on impeller diffuser interactions in radial diffuser pumps to investigate the unsteady flow, and more attention is paid to pressure fluctuations on the blade and vane surfaces Computational results show that a jet-wake flow structure is observed at the impeller outlet. The biggest pressure fluctuation on the blade is found to occur at the impeller trailing edge, on the pressure side near the impeller trailing edge, and at the diffuser vane leading edge, independent of the flow rate, radial gap, and blade number configuration. All of the flow rate, blade number configuration, and radial gap influence significantly the pressure fluctuation and associated unsteady effects in the diffuser pump.

Khalid Y.A. et al[25] (2007) has designed and fabricated wear testing rig to analyse and to select parameter that can be used to determine the wear rates of slurry pump impeller. In his experiments he used an open type impeller made of cast iron with 165mm diameter and five numbers of blades. The slurry used consists of solid- liquid mixture of sand and crushed stones with water. He found out that the weight loss of the impeller is due to the material removal from the impeller as a result of erosion wear. The material is removed from several locations such as circumference, thickness of the blade, height of the blade and depth of the impeller shroud (base). Among these parameters, height loss of the blade represents the highest percentage of 60.86 percent followed by thickness loss of the blade of 35.09 percent, while the diameter loss of the impeller has the lowest loss that is 2.30 percent. All these percentage values are related to the original values.

Further it has also been concluded that the region near the center of impeller encounter less wear compared to the region at the rim of the impeller. The surface topography at the rim of the impeller showed that the materials are removed in the tangential direction to the impeller.

Cheah K. Wet et al[26] (2007) had performed the numerical simulation on impeller of centrifugal pump with six twisted blades. The result showed that the impeller passage flow at design point is quite smooth and follows the curvature of the blade. However, flow separation is observed at the

leading edge due to non tangential inflow condition. For the pressure distribution, the pressure increases gradually along stream-wise direction in the impeller passages. When the centrifugal pump is operating under off design flow rate condition, unsteady flow developed in the impeller passage and the volute casing. Different flow rates were specified at inlet boundary to predict the characteristics of the pump.

Roudnev et al[27] (2007) have observed the erosion wear of casing of slurry pumps and predicted the accurate location of maximum erosion through CFD simulations and experimental data. All 3D simulations predicted similar wear rate magnitudes. It is being estimated that area nearer to upper part of volute casing experiences maximum wear. CFD multiphase simulation using the Eulerian-Eulerian approach is being applied to determine the velocity fields and solid concentration in the centrifugal pump.

Gandhi and Desale [28] (2008) carried out erosion wear tests using seven different ductile type materials namely aluminium alloy (AA6063), copper, brass, mild steel, AISI 304L stainless steel, AISI 316L stainless steel and turbine blade steel using three different erodents namely quartz alumina and silicon carbide which have been mixed with water to prepare three different solid liquid mixtures. Experiments were conducted using a slurry pot tester by orienting the wear specimens normal to their rotational direction. The mean size of erodent was taken as 550µm. Different combinations of erodents and target materials were taken. It was observed that wear at normal impact condition is a strong function of hardness ratio which is defined as the ratio of hardness of erodent and target materials. Experiments were also conducted for different solid concentrations, particle sizes and velocities.

Based on the experimental data Gandhi developed a correlation to estimate the erosion wear rate for normal impact condition.

$$E_{d90}=6.62\times10^{-14}\times K_{(Hp/Ht)}V^{2.02}d^{1.62}C_w^{-0.285} \quad \text{.....(2.3)}$$

where V is the velocity of impacting particle in m/s; d the particle size in _m; C_w the solid particles concentration in wt%; $K(H_p/H_t)$ is a constant, which is a function of the hardness ratio and is express as under,

$$K_{(Hp/Ht)} = 0.42, \text{ for } H_p/H_t \leq 6 \quad \text{.....(2.4)}$$

$K_{(Hp/Ht)}$ = 1.0, for $6 \leq H_p/H_t \leq 12.3$.....(2.5)

And

$K_{(Hp/Ht)}$ = 1.83, for $12.3 \leq H_p/H_t$ .....(2.6)

Gandhi and Disale[29] (2009) had conducted experiments in a pot tester to investigate the effect of particle size on erosion wear of aluminium alloy 6063 (AA 6063). Narrow sized particulate slurry of Indian standard sand (quartz) with mean size varying in the range of 37.5-655μm were used at 3m/s velocity for 20% wt. concentration of solids at 30°-90° orientation angles. Further it was concluded that there exists minimum kinetic energy of the particles, which changes mechanism of material removal from erosion to three body abrasion. Due to three body abrasion, the wear due to smaller sized particles is little higher compared to that of bigger size particles.

Zhou Guanghong and Ding Hongyan[30] (2009) has studied the corrosion–erosion wear behaviours of austenitic stainless steels, 316L and 13Cr24Mn0.44N in water–sand slurry and saline–sand slurry, respectively. The corrosion–erosion wear mass-loss was measured to evaluate the influence of medium and materials. The specimen material was austinised and oil quenched and finally annealed to relieve internal stresses. The wear experiments were performed in a modified solid particle slurry corrosion–erosion wear apparatus.

They calculated the wear in terms of relative wear resistance (ε) and synergism ratio (η) where: -

$\varepsilon = W_s/W_c$, W_s is the mass-loss of 316L; W_c is that of 13Cr24Mn0.44N under the corresponding condition.

And

$\eta = (M_{corr}-M_{water})/M_{corr}$, M_{corr} is the entire mass-loss after corrosion–erosion in the saline–sand slurry; M_{water} stands for the mass-loss after abraded in the water–sand slurry.

Based on the results they concluded that the mass-loss ratio of 316L is always larger than that of 13Cr24Mn0.44N whether in saline–sand slurry or in water–sand slurry. The relative wear resistance increases with the increasing of the impingement velocity and arrives at maximum of 1.6. Both the stainless steels present a positive synergism between wear and corrosion. Further,

the dominant wear mechanism of 13Cr24Mn0.44N is abrasive wear in the water–sand slurry, whereas it becomes abrasive wear associated with little corrosive pitting in the saline–sand slurry. As for 316L, the dominant wear mechanism is also abrasive wear in the water–sand slurry, whereas it becomes abrasive wear associated with corrosive delamination fatigue in the saline–sand slurry.

R.C. Shivramamurthy et al[31] (2009) has conducted experiments to analyse erosive wear mechanisms on Co-based and Ni- based coatings on steel alloy done by laser surface modification at a fixed velocity of 12m/sec and concentration 10kg/m^3 in a test rig and pointed that the erosion rate decreases with the coating and the erosion rate in Ni-based steel is less as compared to Co- based coated steels.

Kalekudithi ekambara et al [32] (2009) the behavior of horizontal solid_ liquids (slurry) pipeline flow was predicted using a transient three dimension hydrodynamic model based on the kinetic theory of granular flow. computational fluid dynamics simulation result obtained using a commercial CFD software package .the simulation were carried out to investigate the effect of in solid volume concentration (8 to 45%),practical size (90 to 500um) mixture velocity (1.5 to 5.5m/s) and pipe diameter 50 to 500mm. and concluded that the CFD model describe here is capable of predicting particle concentration profile for fine particle slurry .it also concluded that when particle are coarse and concentrated profile are primary depends upon the in situ solid volume fraction.

L.J.W. Graham et al[33] (2009) did quantitative analysis of erosion wear behaviour of complex geometries of slurry pipes using CMM method and compared with and compared it with paint modelling, visual observations and CFD erosion modelling. They had observed that CMM technique shows significant promise for obtaining quantitative data for comparison with CFD modelling of erosion. The technique can be used for full scale equipment if a sufficiently large CMM is available.

Sanna Haavisto et al [34] (2009) have studied the particle velocity and concentration profiles of sand-water slurry in a stir tank. Three dimensional velocity profiles were measured utilizing ultrasound Doppler velocimetry along lines located circumferentially between two baffles of the

tank. The volume fraction of the solid phase investigated by them were 5% and 10%. They have conducted CFD studies of slurry flow with algebric slip mixture model and full Eulerian multiphase model. Standard k-ε model was applied in turbulence modelling.The agreement between the simulated and the measured particle velocities was found to be relatively good in the central region of the vessel. Near the wall, deviation of the results was observed with increasing solid concentration. Eulerian multiphase model was tested with parameters corresponding closely to those used with algebraic slip mixture model. Results obtained with it deviated from measurements more than mixture model predictions.

S.L. Liu et al[35] (2010) studied the effect of erosion wear on WC-10Co-4Cr coated steels and the influence of nano-WC–12Co powder addition in WC–10Co–4Cr AC-HVAF sprayed coatings on wear and erosion behaviour. The result showed that 15% addition of nano-WC–12Co has improved the hardness of AC-HVAF coating from 1677 to 1873 HV. It was concluded that the erosion resistance and porosity of WC–Co–Cr coatings increased with addition of nano-WC–12Co content in the cermet coatings from 5 to 15 wt%. This confirmed that adding an appropriate amount of nano-WC–12Co powder has greatly improved the performance of coating.

Cunkui Huang et al[36] (2010) developed a comprehensive phenomenological model for erosion of the material in slurry pipeline flow. The model showed that the erosion rate has a power-law relation with slurry mean velocity, particle size, pipe diameter, fluid viscosity and solid concentration. It has been concluded that the erosion rate strongly depends on mean velocity and weakly on pipe diameter and fluid viscosity. Also the model tells that the effect of particle size on erosion rate depends on the particle shape, flow condition and erosion location on the periphery of a pipe and the value of the exponent of slurry mean velocity varies in a range of 2–3.575, which is found to be consistent with most of the experiments.

CHAPTER 3

STUDY OF PROPERTIES OF BOTTOM ASH SLURRY

3.1 BOTTOM ASH SLURRY

Bottom ash and fly ash are the remains or residue of coal, burning in thermal power plants. Fly ash being lighter in size escapes up the chimney along with the fumes to the atmosphere whereas bottom ash gets settled at the base of the furnace. Bottom ash is coarser than fly ash with grain size spanning from fine sand to fine gravel as shown in figure 3.1**.**

Figure 3.1 Bottom Ash

The different standard methods are used to determine the physical and chemical properties of bottom ash. A brief description of all these tests has been discussed here.

3.1.1 Particle Size Distribution (PSD)

It refers to the variation in the size of solid particles present in the solid sample. SEM image as shown in figure 3.2 shows the particles of different sizes of bottom ash.

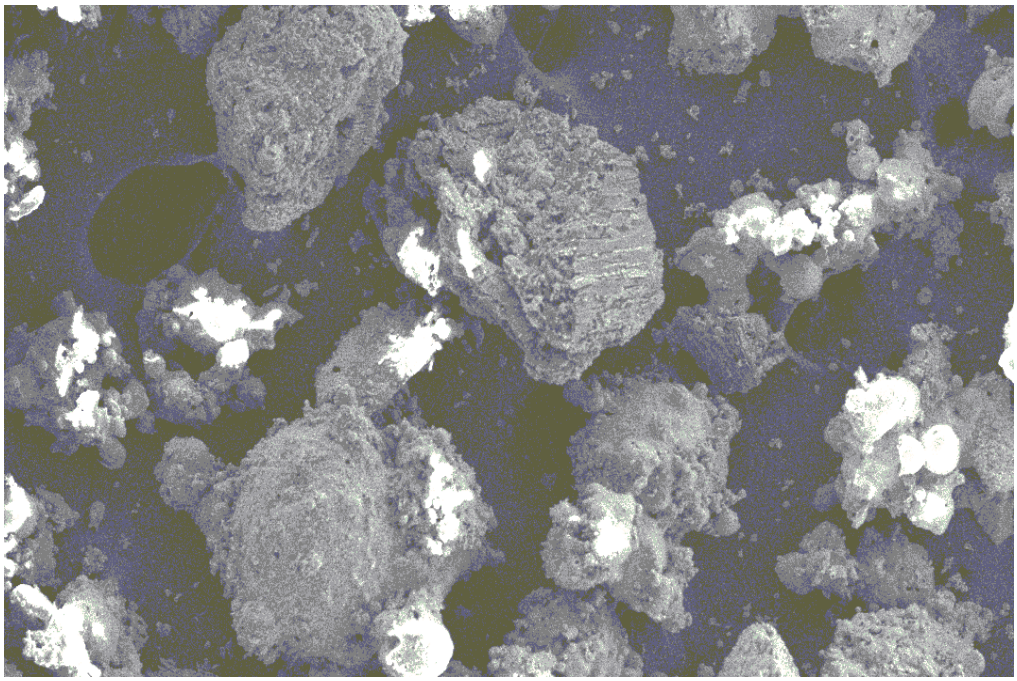

Figure 3.2 SEM image of bottom ash

To determine the distribution of particle size, two methods namely sieve analysis and hydrometer analysis is employed. Sieve analysis is done to determine the particle size of coarse particles which are greater than 75 microns whereas hydrometer analysis is performed for finer particles i.e. below 75 microns.

Figure 3.3 Sieve Shaker

To determine the PSD of bottom ash, a known weight of representative sample of solid particles is taken and washed over a B.S. 200 mesh (75 mm). The material retained over the sieve as well as the finer particulate material are dried in an oven. The dried coarser material is sieved through a set of standard sieves (figure .3.3). Special care is taken to ensure that the sample is properly dried. The sample retained on each sieve is collected and the percentage retained on each sieve is calculated using the standard procedure. The particle size distribution of the fine particles collected (<75 mm) is then determined using the standard hydrometer analysis.

The experimental result of bottom ash is shown in **table 1.1 in (Annexure I).** The variation of particle size is shown in the figure 3.4 below.

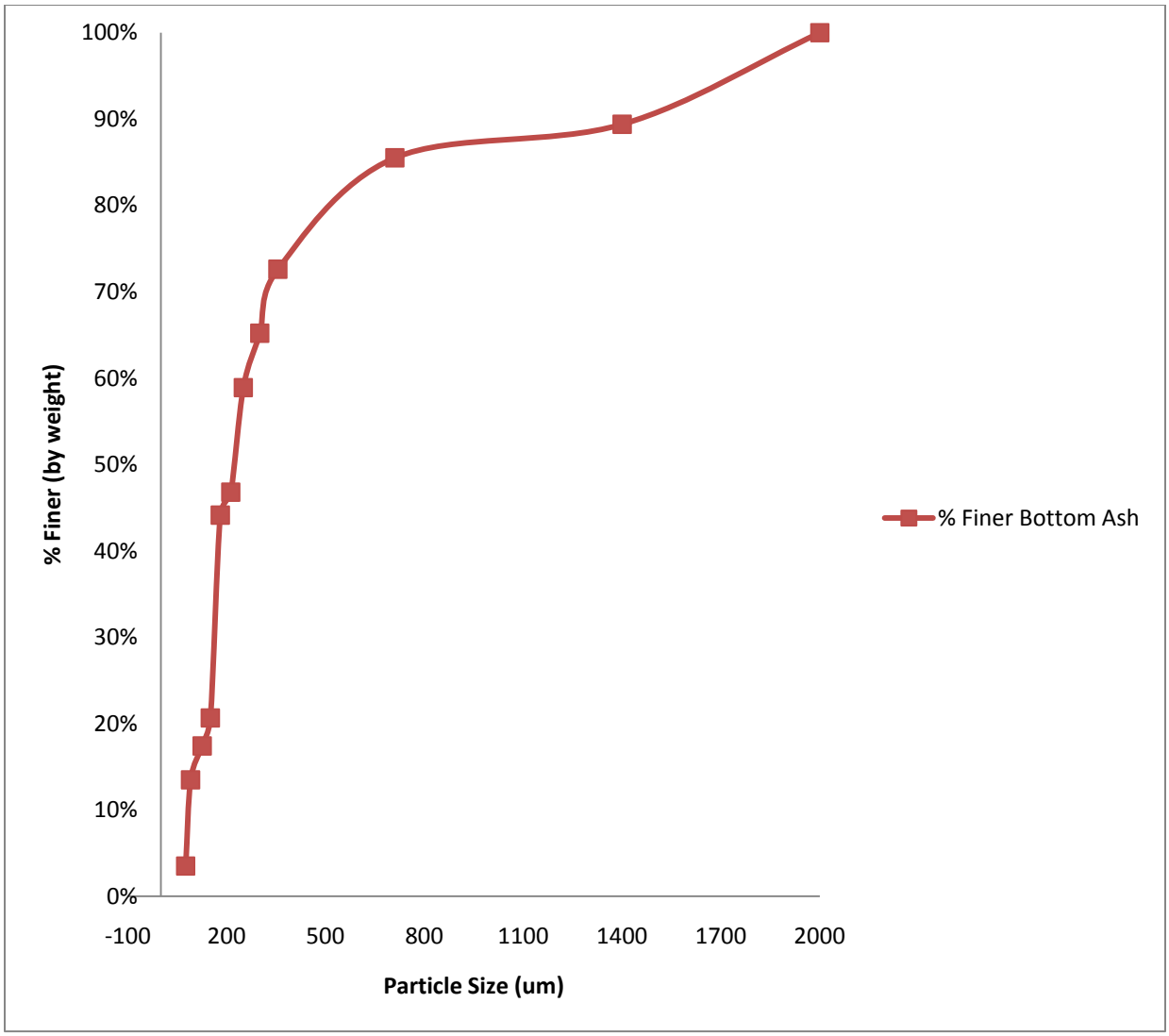

Fig. 3.4 Particle size distribution of bottom ash

3.1.2 Static settled Concentration

The static settled concentration is determined to find out the maximum solid concentration of the slurry obtained by the simple gravitational settling at the static state of the slurry (i.e. no motion of fluid particles). The parameters on which the static settled concentration depends are density and viscosity of the carrier fluid, specific gravity, shape and size distribution of solids etc. In the present study, the static settled concentration of bottom ash slurry of overall 20% concentration (by weight) has been found out. The procedure involved in this method is discussed below.

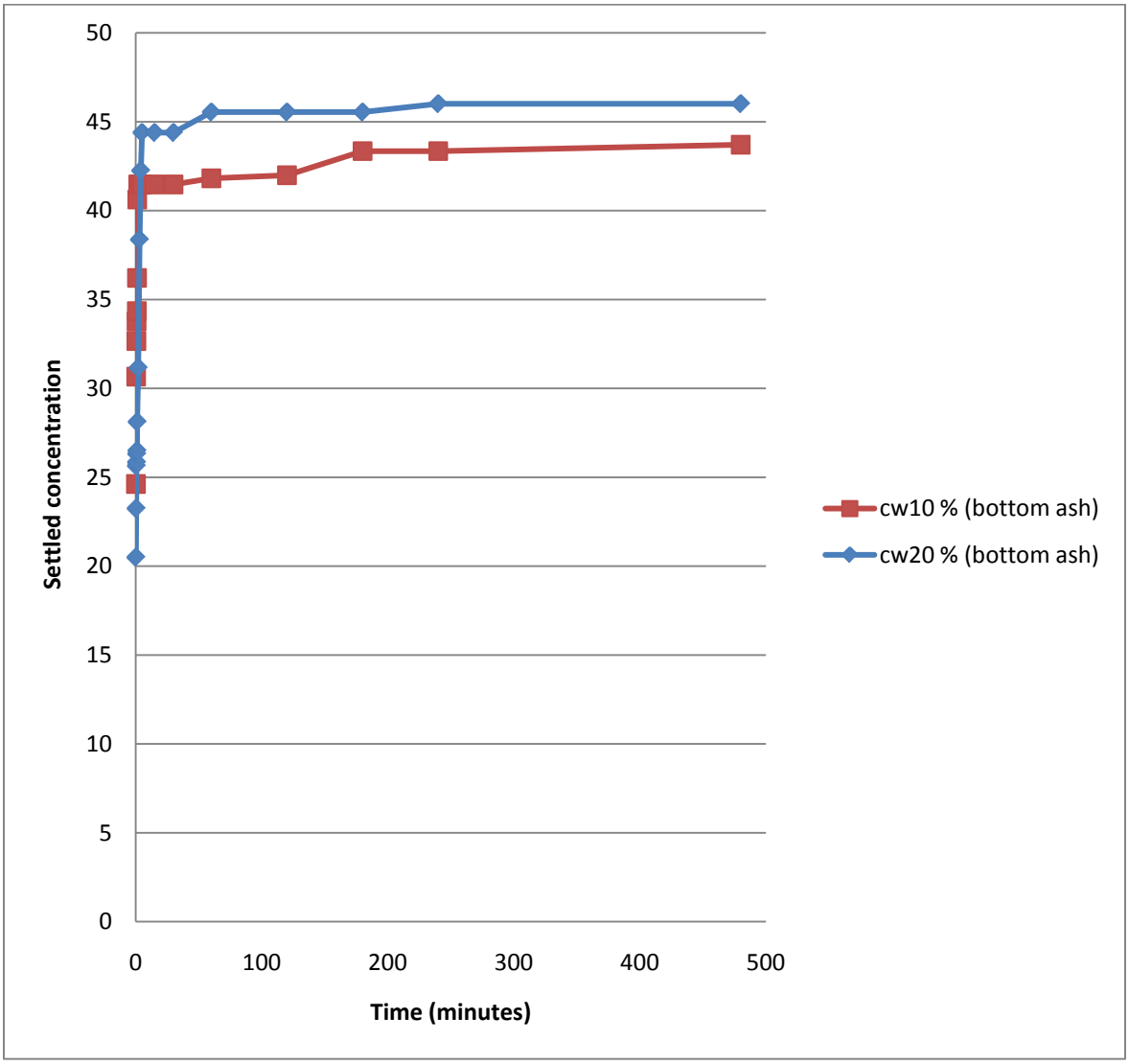

Figure 3.5 Static settled concentration of bottom ash

Take the known amount of bottom ash with water so as to ensure the concentration of 20% by weight. First put the known amount of water in a jar and then put the required quantity of solid in it. Then leave the jar for 2 hours. After 2 hours close the opening of the jar by hand or some source and vigorously mix it by keeping the jar upright.

Note the reading of the level of the ash in the jar with respect to time in each 10 sec. After six readings, increase the interval and take readings in each minute and further increase the interval of reading **(Table 1.2, Annexure II)**. Note the reading until you get the static steady state. The graph is plotted between the static settled concentration and time as shown in figure 3.5.

3.1.3 Specific gravity of Bottom Ash

The specific gravity of bottom ash is determined by the pyknometer test. In this method a 50 ml capacity pyknometer is used. Firstly the pyknometer is cleaned and kept in an oven to remove the moisture content from it. After 2 hours it is taken from oven and cooled down and weighted (W_b). After that small amount of over dried bottom ash (about 30 grams) is put in pyknometer and again weighted (W_{bs}).

Then a small amount of water is poured slowly to ensure that no air is trapped in it and while pouring the mixture is shaken simultaneously. The head of the pyknometer is closed with thumb and mixed vigorously for 5 minutes and then the mixture was kept for 2 hrs to escape the air bubbles formed during the mixing.

After that, completely fill the bottle with water and cork it. Clean the outer surface of the pyknometer and then weight it (W_{bsw}). Now empty the pyknometer, dry it and fill it with distilled water and weight it (W_{bw}). The specific gravity can be calculated by the following formula:

$$\text{Specific gravity} = \frac{(Wbs - Wb)}{\{(Wbw - Wbsw) + (Wbs - Wb)\}}$$

Where,

W_{bs}= Weight of beaker and solid

W_b= Weight of Beaker

W_{bw}= Weight of beaker and water

W_{bsw}= Weight of beaker solid and water.

Table 3.1 Calculation of specific gravity of bottom ash slurry

S.No.	Weight of beaker (Wb) gm	Weight of beaker+solid (Wbs)gm	Wbsw (gm)	Wbw(gm)	Specific Gravity
1	32.4203	62.4135	167.22	150.2513	2.302829283
2	32.7125	62.8465	163.451	146.7528	2.242813975
3	33.4281	63.4375	161.9261	145.2975	2.242720914

Now

Density of solid= Density of liquid× Specific gravity

Table 3.2 Value of density of bottom ash slurry

Specific gravity	**Density of Liquid kg/m^3**	**Density of Bottom Ash (kg/m3)**
2.262788057	**998.2**	**2258.71504**

3.1.4 Rheology

It is the study of deformation and the flow of matter under the action of forces. Transportation of slurry is not as simple as transportation of clear liquids. Many problems come across while transporting slurry through pipelines. These problems often stem from complicated rheological behaviour of the slurry thickening, setting of solids, blocking of the flow, segregations and economic aspects of transportation.

3.1.5 Rheological Measurement

The shear stress-shear rate relationship for slurry can be determined by using Rotating concentric cylinder viscometer. It consists of a fixed cylinder and a rotating cylinder. The liquid is placed between the annular space between the two cylinders and a torque is applied on the rotating cylinder. The slope obtained by the shear stress-strain rate graph will give the viscosity of the suspension. For our experiment a viscometer generally named as rheometer has been used for this investigation as shown in figure 3.6 and figure 3.7.

Figure 3.6 Rheometer

Figure 3.7 Cylindrical cup and rotating bob

The determination of Newtonian or Non-Newtonian behaviour of bottom as slurries has been identified by measuring the variation of shear stress with shear rate at different concentrations. The shear rate is given as an input in the rheometer and corresponding shear stress is obtained. The linear relationship between the shear stress and shear rate graph shows that the fluid is showing the Newtonian behaviour and as it deviates from linear curve, fluid will show the Non-Newtonian behaviour. The experimental results of shear stress and shear rate and relative viscosity at different concentrations has been shown in **table 1.3 and 1.4 (Annexure III)** and the graphs are shown in figure 3.8 and figure 3.9**.**

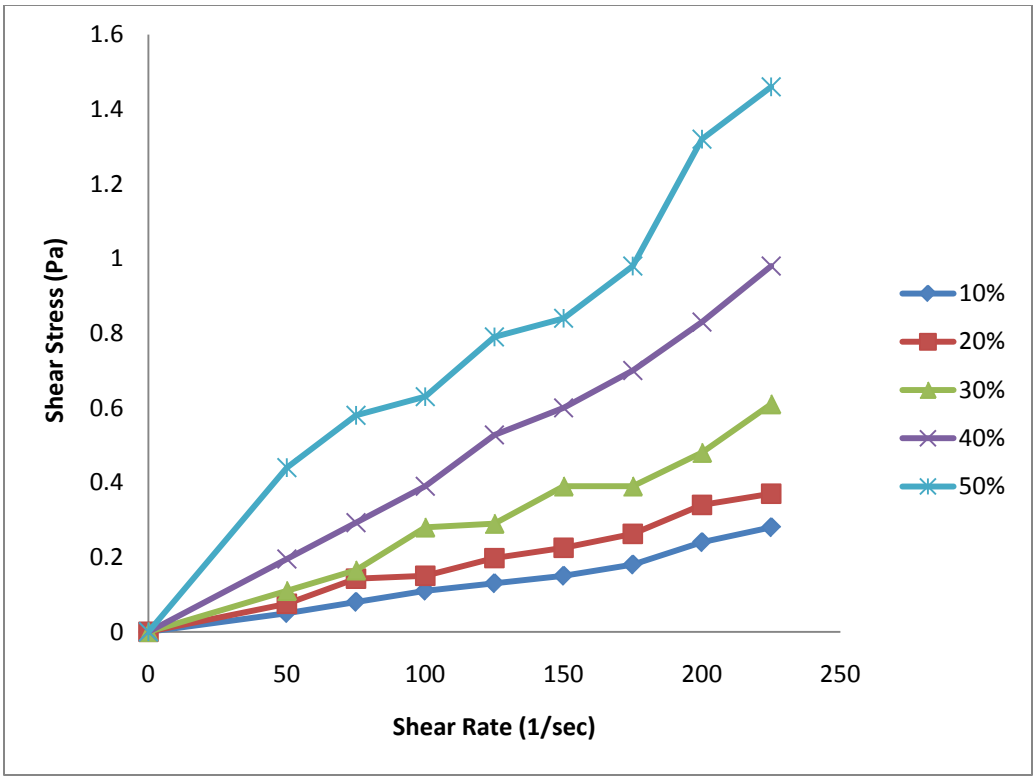

Figure 3.8 Variation of shear stress and shear rate at different values of concentration of bottom as slurry

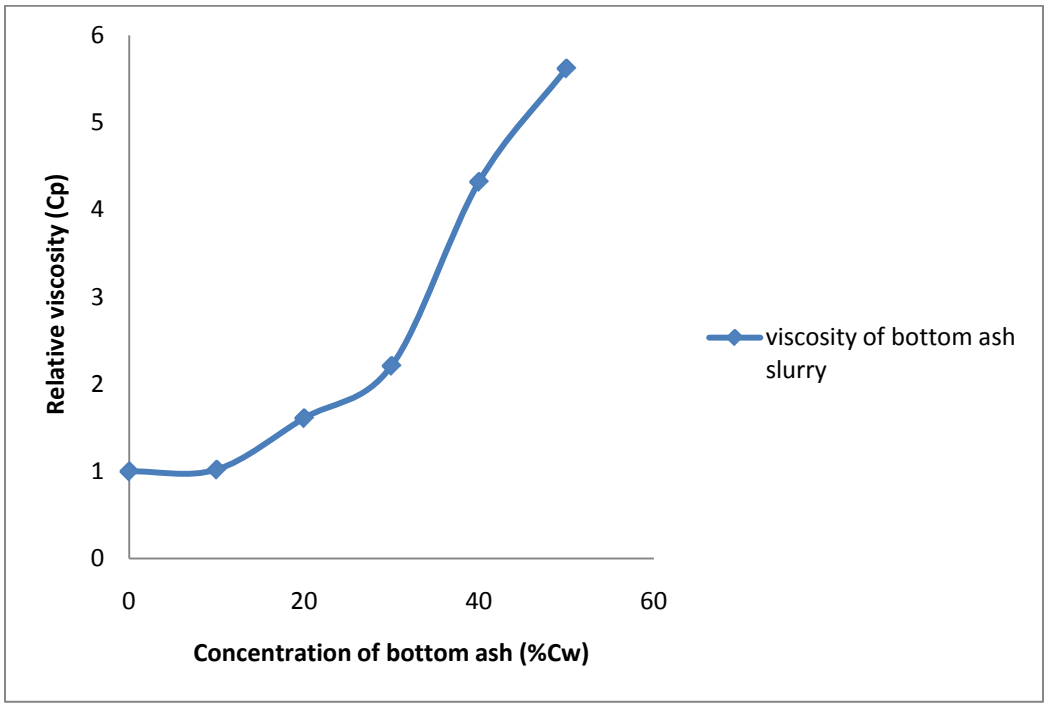

Figure 3.9 Variation of relative viscosity and concentration of bottom ash slurry

3.1.6 pH value

pH value of slurry was determined by using a pH meter at any given solid concentration. The electrode of the meter was first moistened with tap water and then calibrated with a buffer solution of a known Ph value. It is cleaned by rinsing vigorously with distilled water and then immersed in the slurry sample whose pH value was to be determined. The pH suspension was read on the digital display unit when equilibrium value was reached. The experimental results of pH value of bottom ash are shown in **table 1.5 (Annexure III).**

In this test first prepare 7 pH or 4 pH solution dissolve 1 buffer tablet in 100 ml of distilled water. Insert the probe pH meter in the solution and wait for 5 minutes till readings get stabilized. If reading is not equivalent to the pH of solution, then change the control and make the readings equivalent to the pH value of solution. Remove the probe and dip into the distilled water beaker and then dip into the solution or slurry of which PH value is to be determined. Wait for 5 minutes till the reading is stabilized. The variation of pH value with respect to concentration is shown in figure 3.10

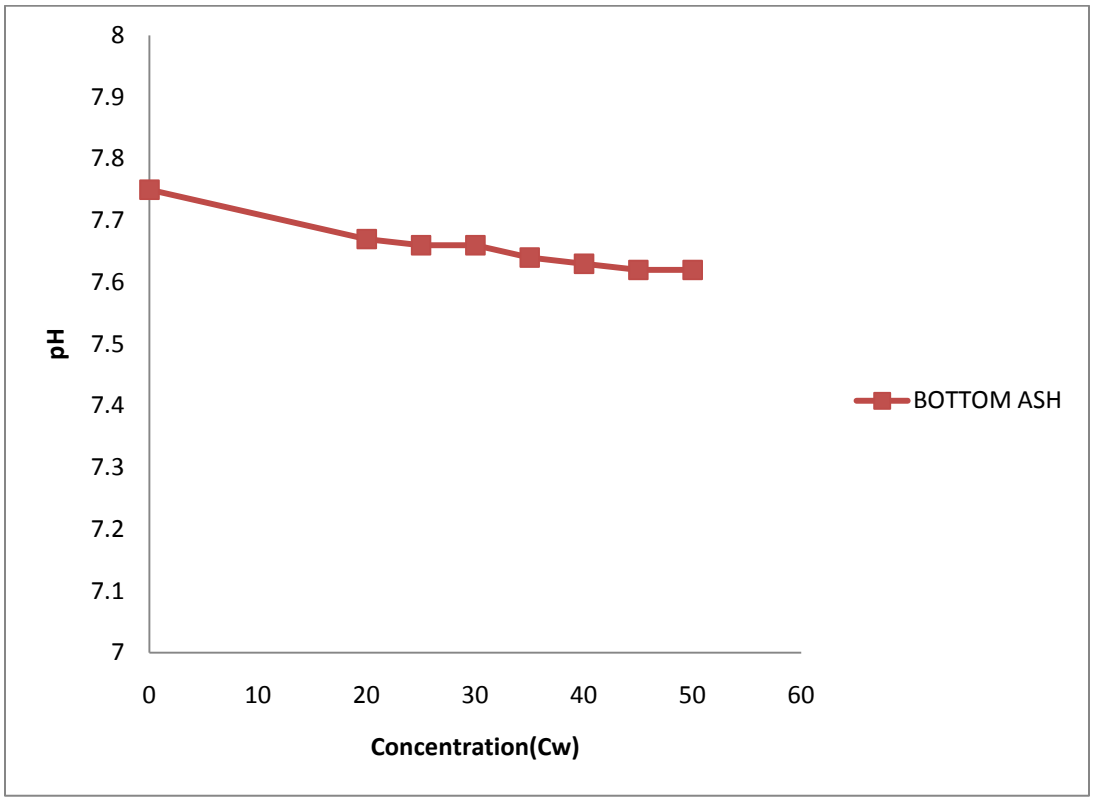

Figure 3.10 Variation of pH value of bottom ash slurry v/s concentration

CHAPTER 4

EXPERIMENTATION

4.1 STUDY OF PROPERTIES OF GREY CAST IRON

Centrifugal pumps used in slurry transportation systems are made up of hard and brittle materials such as grey cast iron, Ni- hard etc. In the present study grey cast iron (ASTM 40) samples are used for estimation of erosion wear.

Basically grey cast iron is a type of cast iron that has a graphitic microstructure. It is named after the gray colour of the fracture it forms, which is due to the presence of graphite. It is the most common cast iron and the most widely used cast material based on weight. It is used for housings where tensile strength is non-critical, such as internal combustion engine cylinder blocks, pump housings, valve bodies, electrical boxes, and decorative castings. Grey cast iron's high thermal conductivity and specific heat capacity are often exploited to make cast iron cookware and disc brake rotors**.** Before conducting the experiments, various properties of grey cast iron were determined.

4.1.1 Chemical Composition

The chemical composition of grey cast iron samples were determined by the spectrometer analysis as shown in figure 4.1. A spectrometer (also known as spectrophotometer, spectrograph or spectroscope) is a device that used to measure the chemical composition of ferrous materials.

The chemical composition is measured by the light intensity produced by arc. A spectrometer is used in spectroscopy for producing spectral lines and measuring their wavelengths and intensities. Spectrometer instruments operate over a very wide range of wavelengths, from gamma rays and X-rays into the far infrared. Figure 4.1, showing the spectrometer.

Figure 4.1 Spectrometer.

The results are given in **table** below

Table 4.1 Spectrometer analysis of grey cast iron

Analysis

Start | New | Print | Del | Store | Recal | Mode | Load | Change | RSD | Exit

Sample: aseem1

Element	Burn 1	Burn 2	Burn 3	Burn 4	Burn 5	Burn 6	Burn 7	Burn 8	Burn 9	Burn 10	Burn 11	Average
Fe %	95.7											95.7
C %	1.88											1.88
Si %	1.35											1.35
Mn %	0.428											0.428
P %	0.0626											0.0626
S %	0.0867											0.0867
Cr %	0.0178											0.0178
Mo %	< 0.0050											< 0.0050
Ni %	0.0943											0.0943
Al %	< 0.0010											< 0.0010
Co %	< 0.0050											< 0.0050
Cu %	0.0247											0.0247
Mg %	0.0006											0.0006
Nb %	0.0210											0.0210
Ti %	0.0191											0.0191
V %	0.0216											0.0216
Pb %	0.146											0.146
Sn %	0.0047											0.0047
B %	0.0079											0.0079
Zr %	0.0202											0.0202
As %	0.0088											0.0088
Zn %	< 0.0050											< 0.0050

Table 4.2 Chemical composition of grey cast iron (ASTM 40)

Composition	Weight Percentage (%)
Fe	94.7
C	2.88
Si	1.35
Mn	0.428
P	0.626
S	0.08
Cr	0.01

4.1.2 Coating of Grey cast iron By Nickel Electroplating

The experiment of the study of erosion wear was performed on both coated and non coated grey cast iron samples. The coating was done by electroplating process of thin layer of nickel on substrate material at Roorkee.

Electroplating can be defined as a plating process in which metal ions in a solution are moved by an electric field to coat an electrode. The process uses electrical current to reduce cations of a desired material from a solution and coat a conductive object with a thin layer of the material, such as a metal. Electroplating is primarily used for depositing a layer of material to bestow a desired property (e.g., abrasion and wear resistance, corrosion protection, lubricity, aesthetic qualities, etc.) to a surface of the material. The anode and cathode in the electroplating cell are both connected to an external supply of direct current — a battery or, more commonly, a rectifier. The anode is connected to the positive terminal of the supply, and the cathode (article to be plated) is connected to the negative terminal.

When the external power supply is switched on, the metal at the anode is oxidized from the zero valence state to form cations with a positive charge. These cations associate with the anions

in the solution. The cations are reduced at the cathode to deposit in the metallic, zero valence state.

In the present work, nickel plate is placed at anode and cast iron sample at cathode in a bath of nickel sulphate. As shown in figure 4.2**,** nickel is oxidized at the anode to Ni^{2+} by losing two electrons. The Ni^{2+} associates with the anion SO_4^{2-} in the solution to form nickel sulfate. At the cathode, the Ni^{2+} is reduced to metallic nickel by gaining two electrons. The result is the effective transfer of nickel from the anode source to a grey cast iron plate covering the cathode.

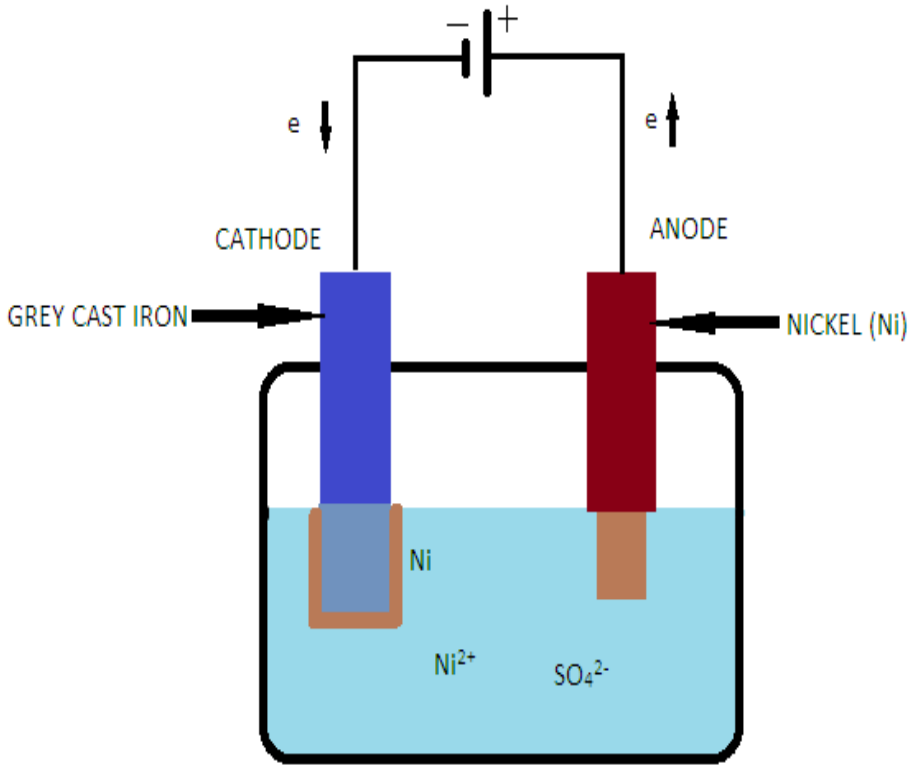

Figure 4.2 Nickel electroplating on grey cast iron specimen.

4.1.3 Microhardness

Figure 4.3 Display of indent

Figure 4.4 Micro hardness equipment

Micro hardness tester (as shown above) was used to estimate the hardness of specimens with and without coating. The load applied was 300mg and VHN values were determined by applying this load by using a calibration distance of 50 units in quantinet software as shown in figure 4.3 and figure 4.4 used for image analyzing. The dwell time used during load application was 25 seconds.

The microhardness of uncoated grey cast iron was found to be 245 VHN and that of coated was 472 VHN.

4.2 EXPERIMENTAL SET UP

The experiments have been performed using a jet impingement tester (Figure 4.5) in which a jet of slurry is subjected to a flat surface of the test specimen and the mass loss of the specimen is measured to identify the erosion of the surface. It consists of a slurry tank in which the required amount of slurry is poured. This slurry is lifted up by means of the centrifugal pump as shown in figure and transferred in the form of jet through connecting pipes. The flow rate of the jet is measured by the electronic magnetic flow meter situated before the jet nozzle along the pipe. The volume of water ash slurry flowing through the pipe is controlled by the by pass valve situated before the magnetic flow meter. The maximum flow rate in the jet erosion tester can go up to 3.5l/sec and the maximum concentration is 3% by volume. The specimen is fixed in a slot which can be rotated at three different impact angles of 30°, 60°, and 90° respectively relative to the direction of the jet. Slurry flowing through the pump at high pressure is converted into high velocity stream while passing through the converging section of the nozzle, which is 125mm long, and having diameter of 8 mm. The standoff distance between the nozzle and specimen can be varied from 25mm to 90mm. The slurry falls back into the tank after striking to specimen. The holder is located on the top of tank enclosed in a casing made of steel angle and fitted with fiber sheet, to facilitate the removal and clamping of the specimen.

The electronic magnetic flow meter (Elmag-200M) arranged (as shown in figure 4.1) in between control valves and nozzle, is equipped with digital display and contains PTEF coated liner through which the slurry flows and discharge is calculated, when a conductive fluid passes through magnetic field (applied) a voltage is induced in an electrically conductive body which is proportional to the mean flow velocity according to Faraday's law of induction. The components of erosion jet tester are as follows.

(1) Centrifugal pump

(2) Electronic magnetic flow meter

(3) Nozzle and Holder assembly

(4) Conical Tank

Figure 4.5 Experimental Set up

4.3 PREPARATION OF WEAR SAMPLES BEFORE EXPERIMENT

The following steps are involved in preparing the wear samples before wear tests:

Prepare wear samples of dimension as per the provision of slot in the fixture. The next step is polishing. To enable proper polishing, mount the specimens appropriately (glue it with feviquick on a flat surface object) if they are of small size. Polish the specimen in sequence with 200, 400, 500, 600, 800 and finally with 1000 grade sand paper.

Make sure that the hand pressure is maintained uniform while polishing so that the surface polished is perfectly flat. If the surface is not flat then micro hardness readings will not be accurate. After polishing with sand paper, polish it with fur cloth. Sample is ready for wear tests.

4.4 EXPERIMENTAL PROCEDURE

As discussed above, the wear specimens both coated and uncoated were prepared for the experimental analysis. The concentration of the slurry was kept constant as 3% by volume and the particle size was below 150 microns. The two parameters namely impact velocity (or flow rate) and impact angle were varied for determination of erosion wear. The range of the impact angles was 30° to 90° in step of 30° at three flow rates namely 1.75l/sec, 2.6l/sec and 3.5l/sec respectively. The specimen was fixed in the slot at a certain angle and the jet was subjected at a certain flow rate for one hour and the mass loss of the specimen was noted. For a particular angle and flow rate the experiments were conducted for four hours and readings of the mass loss (in mg) of the specimen were noted after every one hour. Different samples were used for taking readings at different angles and flow rate respectively. In this way readings of the mass loss were taken at each angle corresponding to each flow rate. The erosion wear of both coated and non coated grey cast iron samples were measured in the form of mass loss of the specimen.

CHAPTER 5

DESIGN OF POT TESTER

Erosion pot tester is to be designed to overcome the limitations of the erosion jet tester. The limitation of the erosion jet tester is that the slurry concentration cannot be increased more than 3%. But in slurry transportation systems the concentration of slurry up to approximately 40% and hence it is difficult to study the slurry erosion behavior with variation of concentration. So it is needed to design a pot tester to overcome this limitation. Therefore an attempt has been made to model a slurry erosion pot tester which can simulate the erosion wear behavior of slurry handling components. The advantages of slurry pot tester are as follows

- It can be used for high concentration up to 40%
- It is simple in design and easy to operate

The drawing details of the slurry pot tester are discussed below.

5.1 BASIC SKETCH OF EROSION POT TESTER

The pot tester consists of a cylindrical aluminium tank having height 337.5 mm with inner diameter 360mm. A transparent acrylic sheet is used to cover the top of tank. Four full-length baffles are provided at the inner wall of the cylindrical tank at equal distances. The pot tester is provided with two shafts, upper shaft and lower shaft as shown in figure 5.1. The upper shaft is attached to the bench scale drilling machine. The brass sleeve of 45 mm length and 37 mm attached to this shaft at he lower end is used for fixing two horizontal arms to hold two test fixtures at 213 mm distance at diametrically opposite ends inserted from top to rotate the wear specimen inside the slurry pot. Lower shaft is provided from the bottom to rotate a pitched turbine blade propeller for keeping the solid–liquid mixture under suspension. Each shaft is rotated by an independent 1.5 kW dc motor through-belt pulley drive. Each test fixture is fastened with the help of 4 mm screw on the horizontal arm through its one end. Two fixtures are fitted 180° apart to balance the dynamic forces. The fixtures are made of high chromium high carbon steel and hardness of≈ 65 RC was achieved by proper heat treatment. A wear specimen of size of 45mm× 7.5 mm × 3 mm was glued inside the fixture groove.

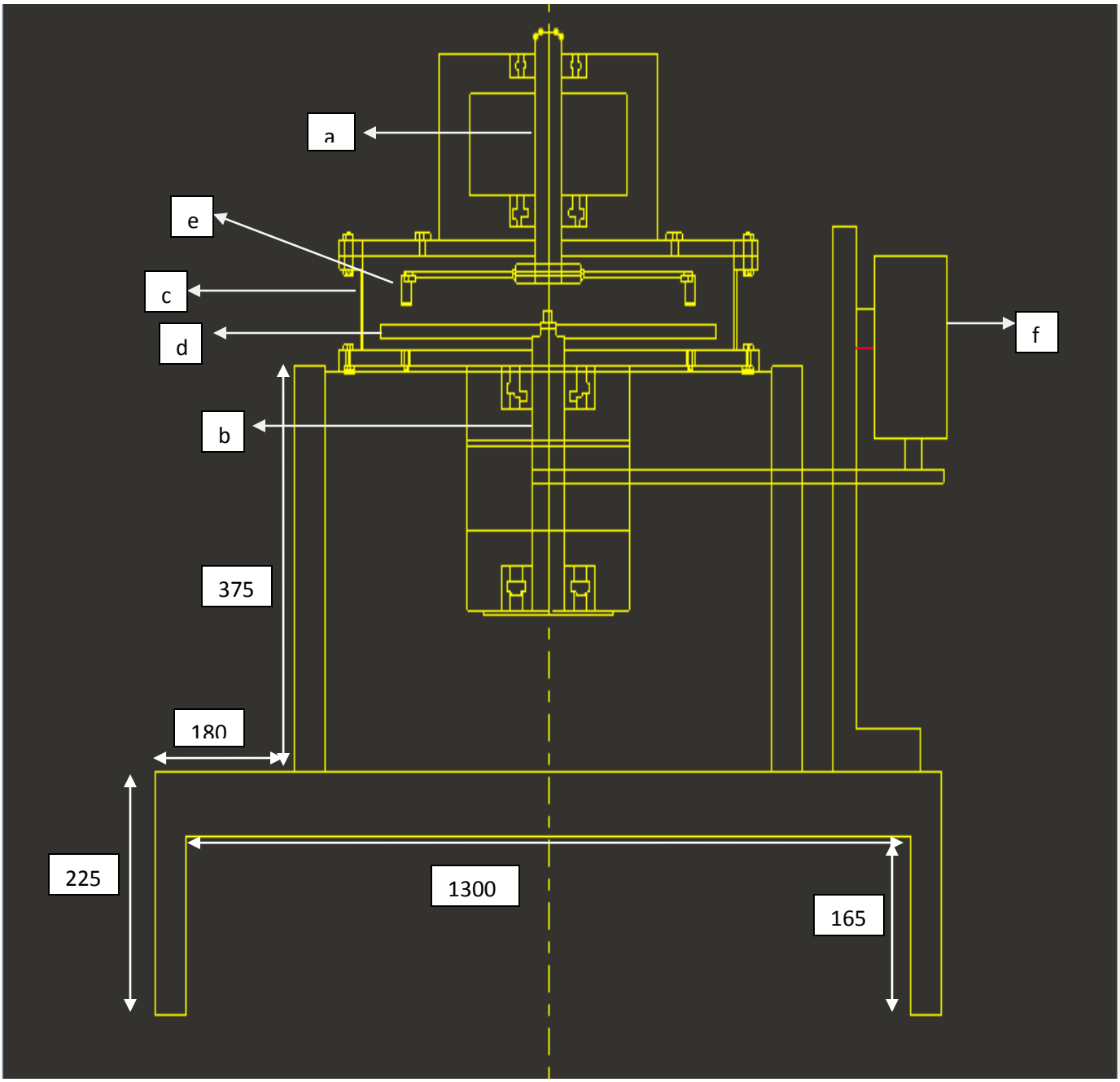

Figure 5.1 Schematic representation of erosion pot tester. (a) Upper shaft (b) lower shaft (c) cylindrical tank (d) propeller (e) wear specimens (f) DC motor. (All dimensions in mm)

A slotted angular plate is fixed on each arm to orient the test fixture at any angle in the range of 0–90° (in steps of 15°) to the tangential direction of rotation. The wear specimen has been rotated at the desire speed in direction opposite to the propeller rotation.

The speed control unit is located to control the speed of both the motors used for running the wear specimens and the propeller. The different components of the erosion pot tester are discussed below in detail.

5.2 COMPONENTS OF EROSION POT TESTER

5.2.1 Drilling machine

A normal heavy duty bench scale drilling machine as shown in figure can be used to rotate the shaft attached to the wear specimens. The specifications and figure of the machine is given in figure 5.2 and table 5.1 respectively.

Figure 5.2 Bench scale drilling machine

Table 5.1 Specifications of drilling machine

Spindle center to column	10 inch 254 mm
Spindle Travel	7 inch 177 mm
Size of table square	19 inch × 482 mm
Size of table round	15 ½ inch 393 mm
Overall height of machine	68 inch 1750 mm
Maximum distance spindle to base	40 inch 1016 mm
Column Diameter	3 inch 108 mm
Machine Base	26 inch × 18 inch × 4 inch × 660 × 457 × 101 mm
Spindle Nose Bore	No. 3 M. T. 4 M. T.
Speed Range	(8) 90 × 2265 R.P.M
Motor speed	1440 R.P.M
Motor	1.5 H.P.
V Belt	V Belt B-55
Weight of machine without motor	260 Kg. (Approx)

5.2.2 Speed Control Unit

The speed control unit will be installed to control the speed of both the motors attached to rotate the wear specimens and the propeller respectively. The rpm of the motors is measured by the magnetic sensors (figure 5.3).A magnetic sensors are fixed at the propeller motor and the drilling motor for measurement of the RPM of both propeller shaft and shaft attached with the specimen holder. The sensor works on the principle of varying magnetic field and generates pulses at every rotation of the motor shaft. Sensors are connected with a control unit panel which displays the RPM. The RPM can be adjusted to the desired value by moving the knob on the control panel.

Figure 5.3 Speed control unit and magnetic rpm sensor

5.2.3 Cylindrical tank

A cylindrical aluminium tank in which the slurry is contained is fixed at the bottom of the shaft attached with the drilling machine. The height of the tank is 337.5 mm and inner diameter is 360 mm. The wall thickness of the cylinder is 5 mm and it is provided with four baffles of 337.5mm X 39mm X 4.5 mm along two orthogonal diametric planes inside the cylinder periphery to break the vortex motion of the slurry at high rpm speeds of the propeller. The PRO-E modeling of the cylindrical tank is shown in figure 5.4. At the base of the cylinder a whole is provided to drain out the slurry.

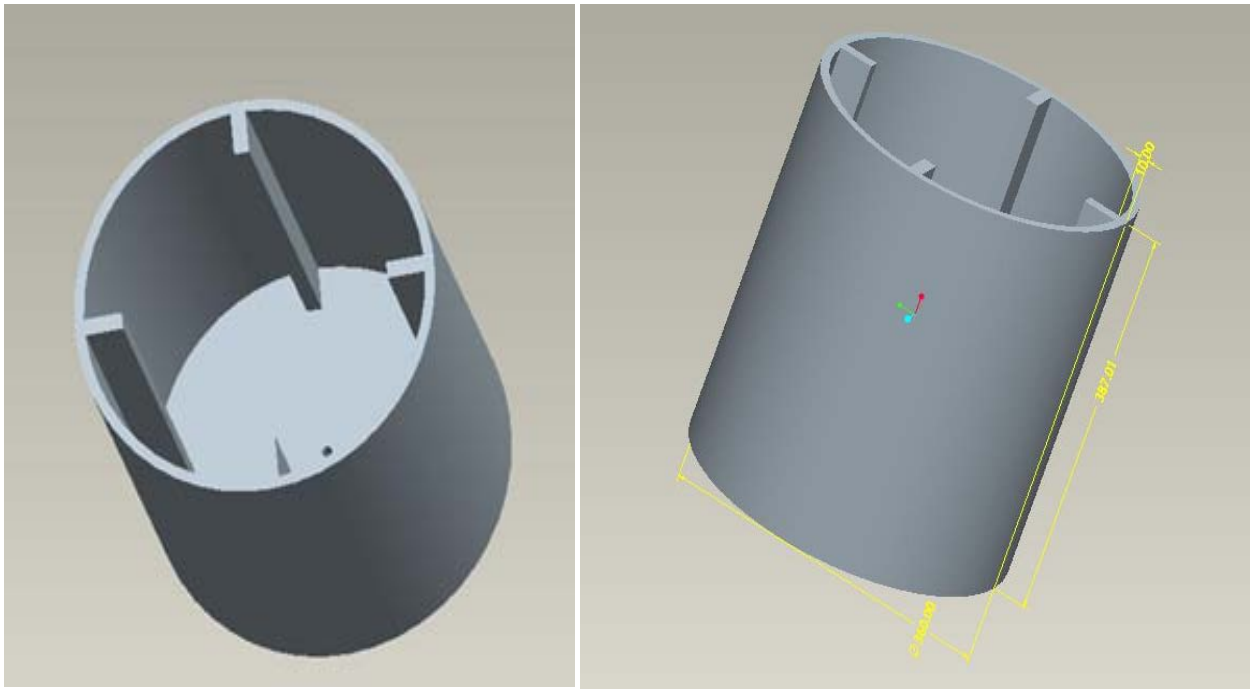

Figure 5.4 Solid model of cylindrical tank

This aluminium tank is fixed on an iron-frame structure, similar to suspension study, with the help of nut-bolts and is covered by a transparent acrylic sheet at the top. A shaft is also inserted from the top of the tank through the transparent sheet to rotate the wear specimens at desired speeds by a separate 1.5 kW DC motor of (drilling machine) through V belt-pulley drive.This shaft is also supported by two bearings mounted in an aluminium block and an oil seal is used to prevent the leakage from the top, if any.

5.2.4 Propeller

A four blade PBT propeller was modeled and a local coordinate axis was created in order to rotate the impeller blades at 45 degrees on their respective axis. The dimensions of the propeller blades are given in the figure 5.5.

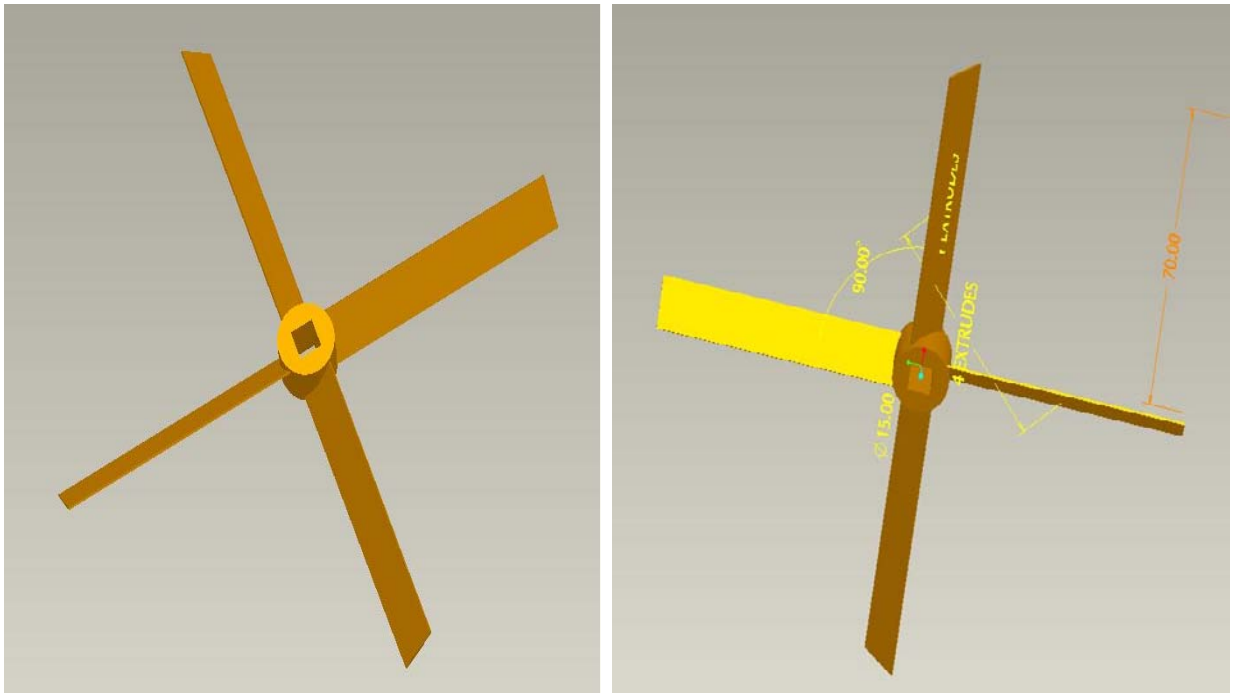

Figure 5.5 Solid model of 45º PBT propeller

A shaft of 16.5mm diameter is inserted from the tank bottom to rotate this propeller inside the tank and is sealed with oil-seal to prevent leakage of solid-liquid mixture. This propeller is rotated inside the tank to keep uniform suspension of solid-liquid of solid liquid mixture inside the cylindrical tank. The propeller can be rotated in both up pumping and down pumping mode

5.2.5 Assembly of cylindrical tank

The assembly of the cylindrical tank after insertion of propeller is shown in figure 6.6. The propeller rotates in the cylindrical tank by means of shaft attached to the dc motor thorough belt and pulley arrangement.

Figure 5.6 Assembly of propeller and cylindrical tank

5.2.6 Test specimen holder

At the lower end of the upper shaft attached with the drilling machine a brass sleeve of 45 mm length and 37.5 mm diameter is provided with provision for fixing two horizontal arms to hold two test fixtures at diametrically opposite ends. Special test fixtures, as shown in Figure 5.7 are designed to mount flat wear specimens.

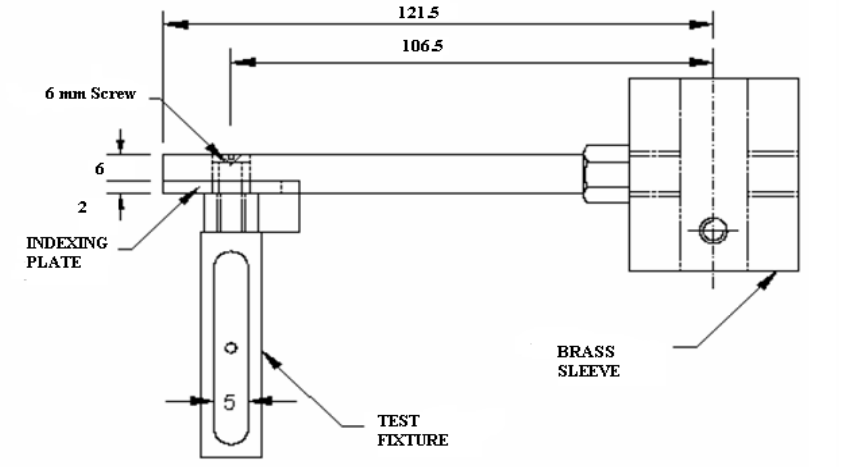

Figure 5.7 Test specimen holder

A slot of size 45 mm x 7.5 mm x 3 mm, rounded at two ends, is provided at the test fixture to fix a wear specimen inside it . A rectangular tooth of 1 mm thickness and 2.5 mm width is provided on each fixture to place it at the required angle from 0 to 90º, in steps of 7.5/15º, with respect to the direction of peripheral velocity, using the slotted angular plate. Two fixtures were fitted at 180º apart to balance the dynamic forces, if any, with minimum wake interference effect.

5.3 COST ESTIMATION

The approximate estimated cost required to fabricate the apparatus is given below in table.

Table 5.2 Cost estimation of erosion pot tester

Components	Estimated Cost (in Rs)
Heavy duty bench scale drilling machine	35,000-40,000
Speed control unit	22,000-25,000
Two RPM sensors	4,000
1.5 KW dc motor	10,000-12,000
Cylindrical tank, propeller, shaft assembly and test fixtures etc,	15,000 (app.)
Installation and fabrication charges	15,000 (app.)
TOTAL ESTIMATED COST	92,000-1,11,000

CHAPTER 6
RESULTS AND DISCUSSIONS

6.1 RESULTS OF EROSIVE WEAR

The results obtained in the experiment has been shown graphically showing the variation of mass loss with respect to impact angle and impact velocity for both coated and uncoated grey cast iron specimens. The flow rate (l/sec) was converted in terms of velocity (m/sec) and the results were shown in terms of impact velocity instead of flow rate.

6.1.1 Erosion wear of grey cast iron at different impact angles

The rate of erosion wear in terms of mass loss with respect to time at different impact angles is shown from figure 6.1 to figure 6.3 table is given in **Annexure IV.**

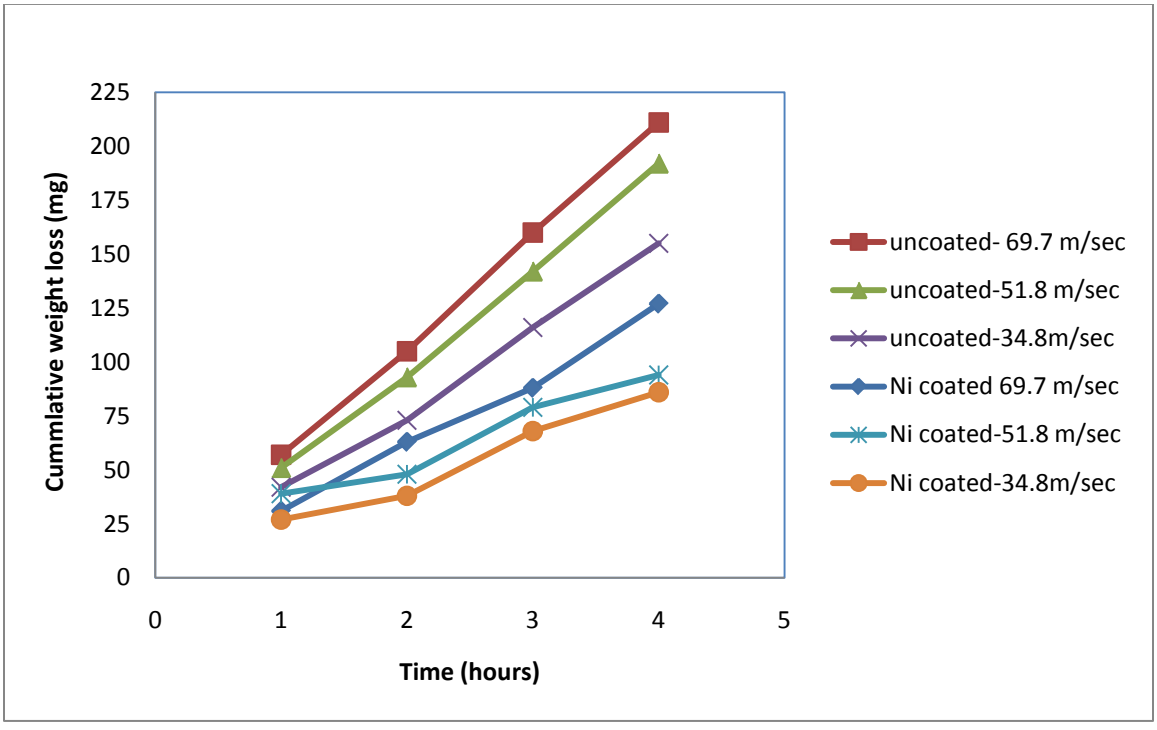

Figure 6.1 Variation of cumulative weight loss v/s time at impact angle of 30°

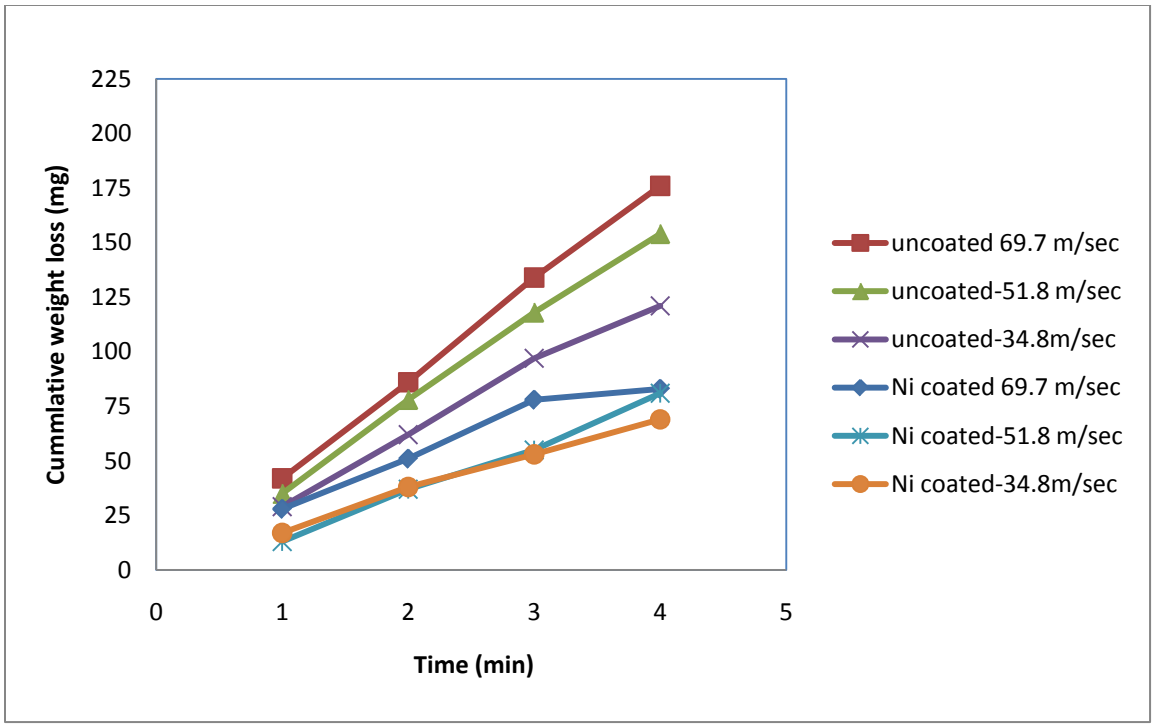

Figure 6.2 Variation of cumulative weight loss v/s time at impact angle of 60°

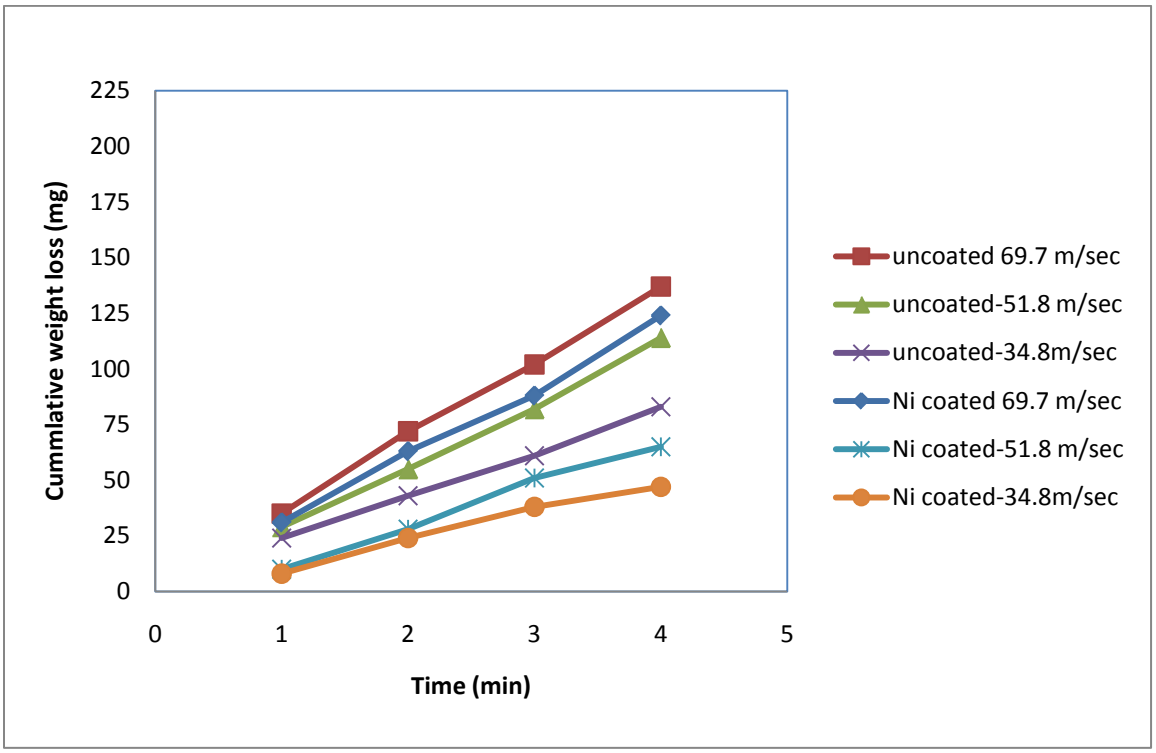

Figure 6.3 Variation of cumulative weight loss v/s time at impact angle of 90°

In figure 6.1 to figure 6.3 it has been observed that the erosion wear in terms of mass loss increases with decrease in impact angle. It is maximum at 30º and minimum at 90º. This may be happened due to the brittle nature of the grey cast iron wear specimen in which phenomenon of erosion wear due to scratching mechanism is pre dominant than deformation and at lower impact angles wear is mainly due to scratching mechanisms.

6.1.2 Erosion wear of grey cast iron at different impact velocities

The rate of erosion wear at different impact velocities with respect to time is shown from figure 6.4 to figure 6.8 and table is given in **Annexure IV.**

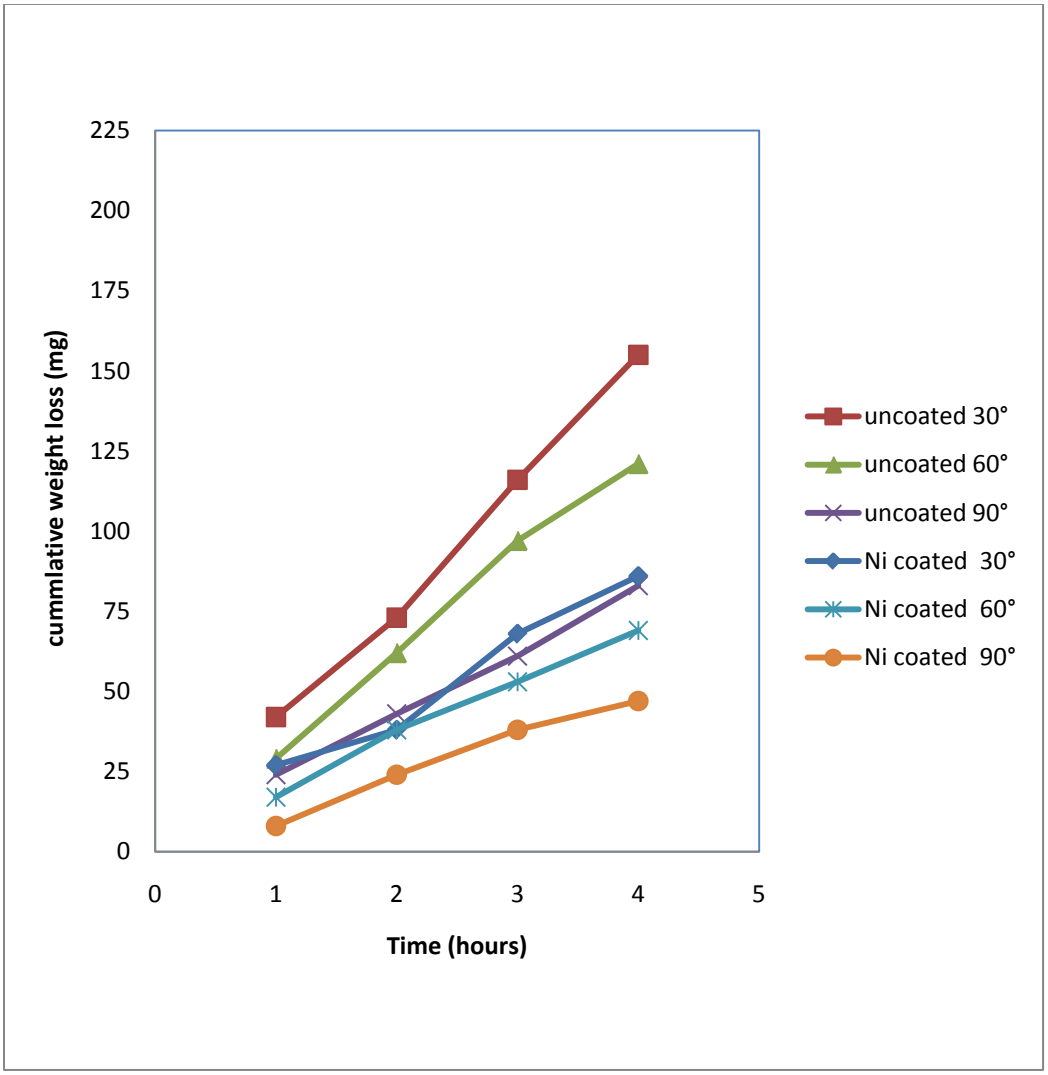

Figure 6.4 Variation of cumulative weight loss v/s time at 34.8m/sec velocity of flow

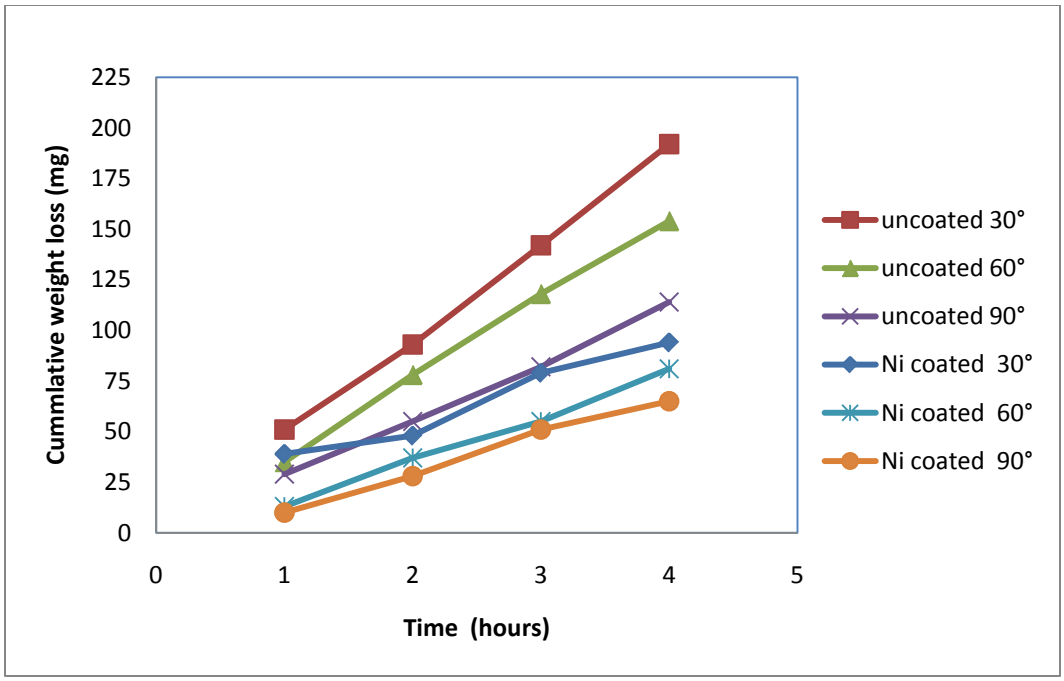

Figure 6.5 Variation of cumulative weight loss v/s time at 51.8 m/sec velocity of flow

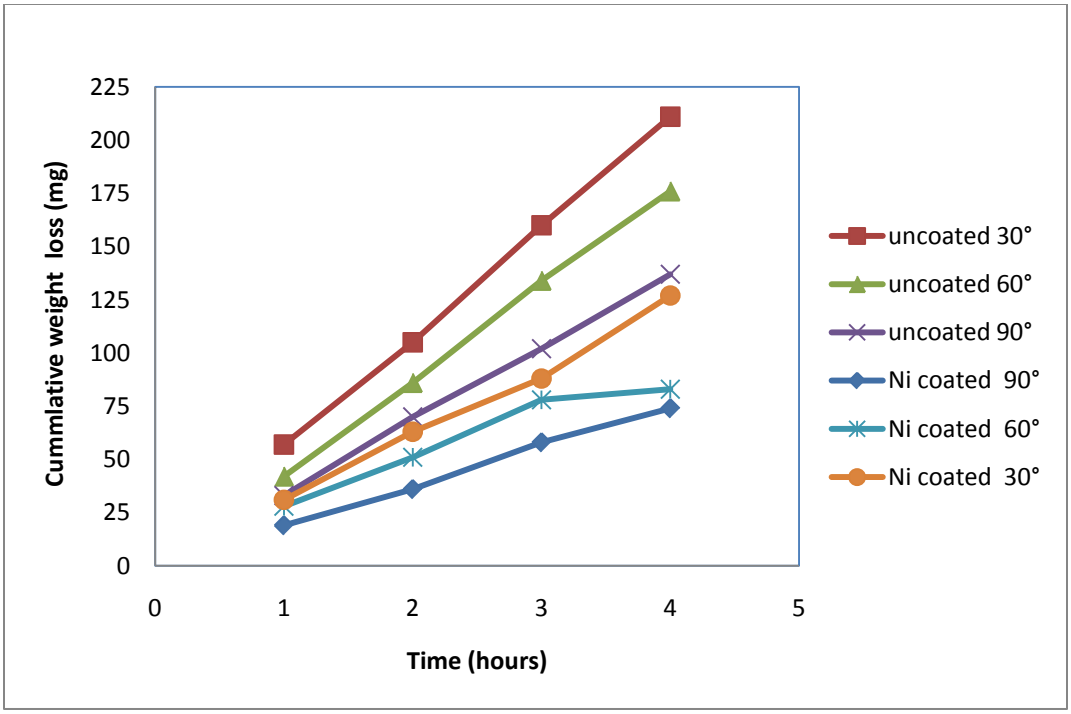

Figure 6.6 Variation of cumulative weight loss v/s time at 69.7 m/sec velocity of flow

From figure 6.4 to figure 6.6 it is clearly visible that erosion wear in terms of weight loss is directly proportional to the flow velocities. It is maximum at the flow velocity of 69.7 m/sec and minimum at the flow velocity of 34.8 m/sec. This due to the fact that high velocities impart high energy which causes the erosion of material from the surface of the grey cast iron specimen.

Also in both cases of impact angle and impact velocities, the erosion wear of Ni- coated grey cast iron specimen is almost 50% decreased as that of uncoated one. Hence it can be said that the coating technique gives better results towards erosion resistance and it can be proved good to be of use to reduce the erosion wear or increase the erosion wear resistance of the pump material.

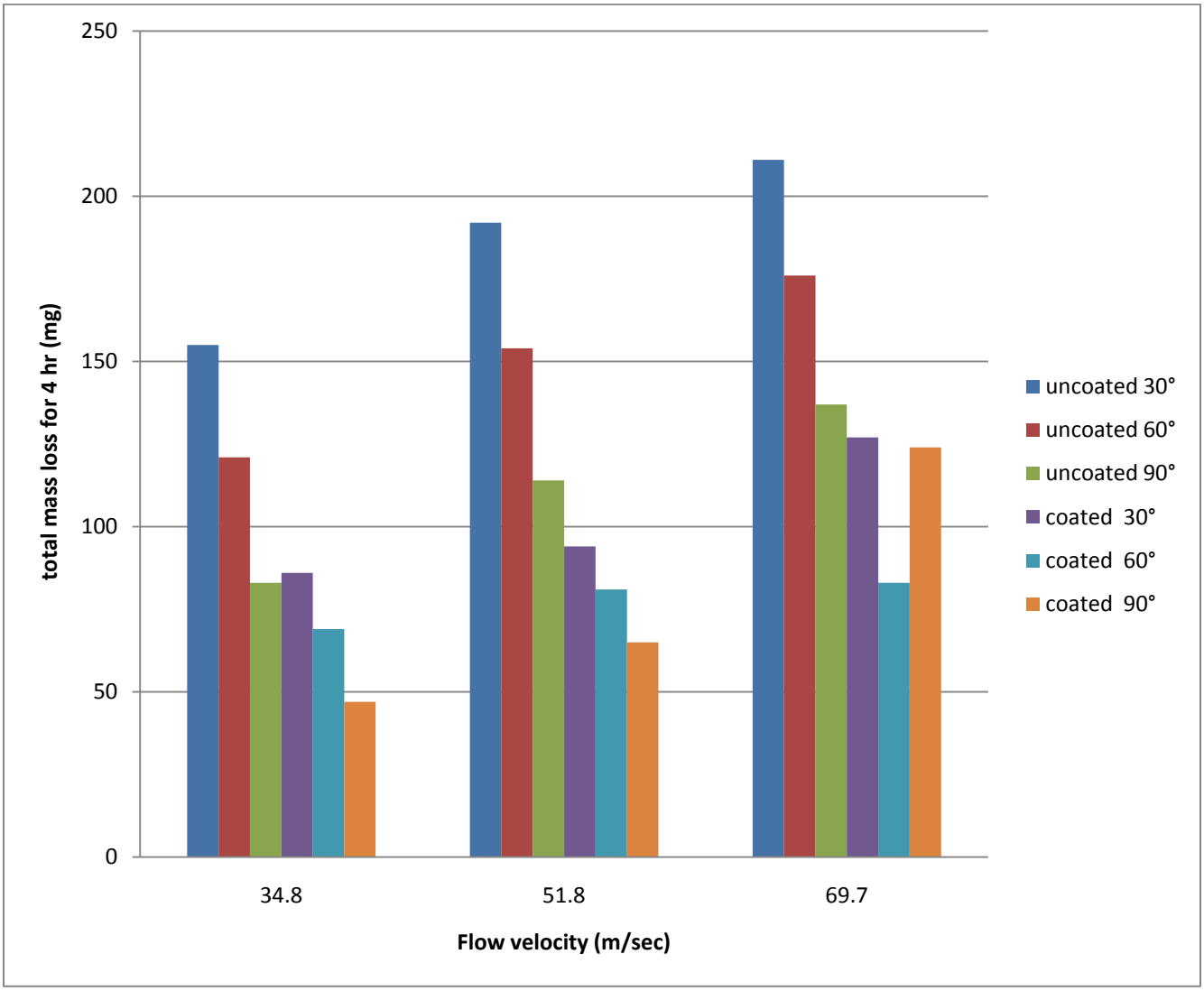

Figure 6.7 Variation of weight loss v/s flow velocity

6.2 SCANNING ELECTRON MICROSCOPE TESTING (SEM)

The scanning electron microscope tester figure 6.8 is used for determination of pattern of wear at the surfaces of the grey cast iron specimen. A scanning electron microscope (SEM) is a type of electron microscope that images a sample by scanning it with a high-energy beam of electrons in a raster scan pattern. The electrons interact with the atoms that make up the sample producing signals that contain information about the sample's surface topography, composition, and other properties such as electrical conductivity.

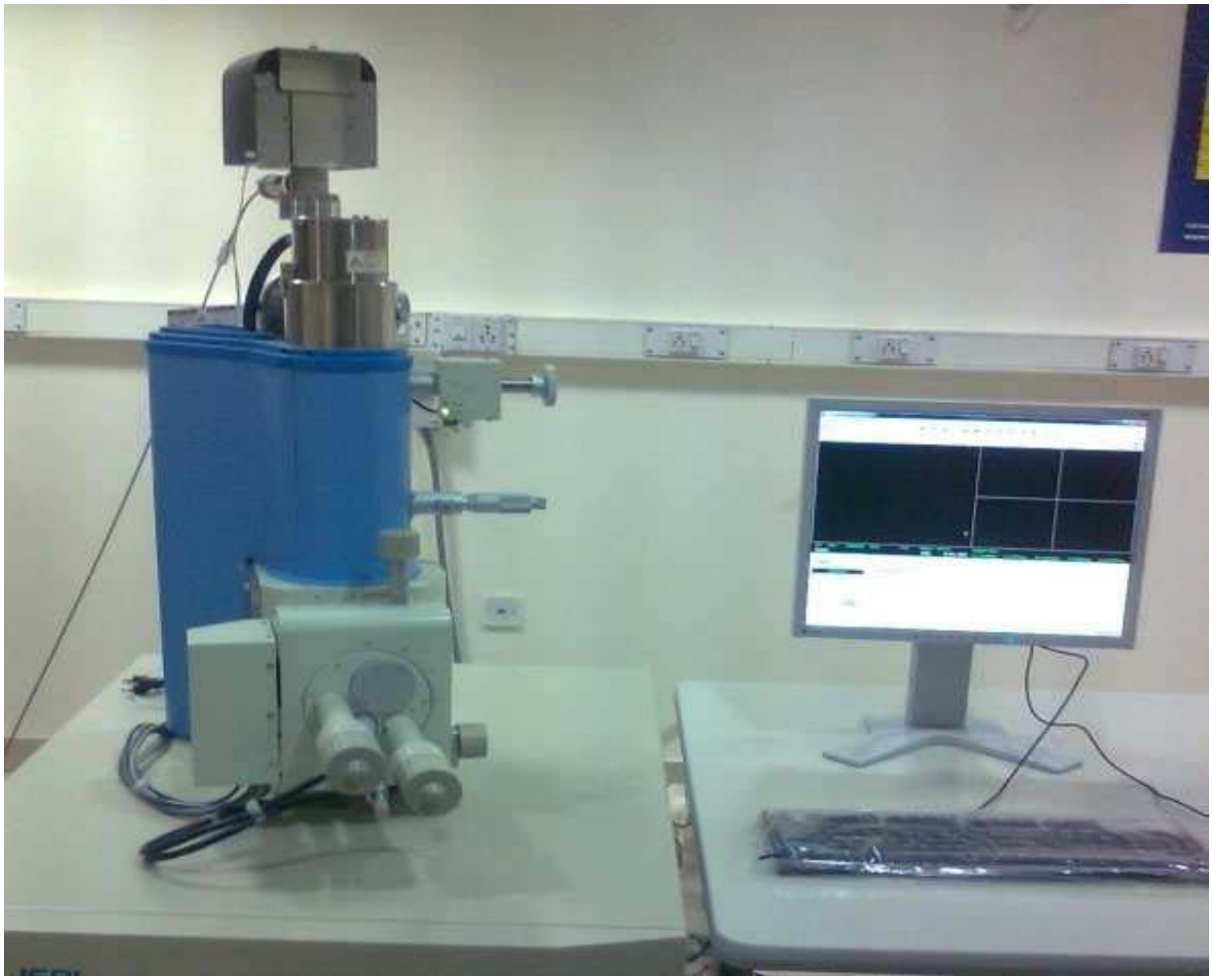

Figure 6.8 Scanning electron microscope

The SEM images of the wear surfaces of both coated and uncoated grey cast iron specimen were taken at 100X, 250X and 500X magnification as shown in figure 6.8, figure 6.9, figure 6.10, figure 6.11.

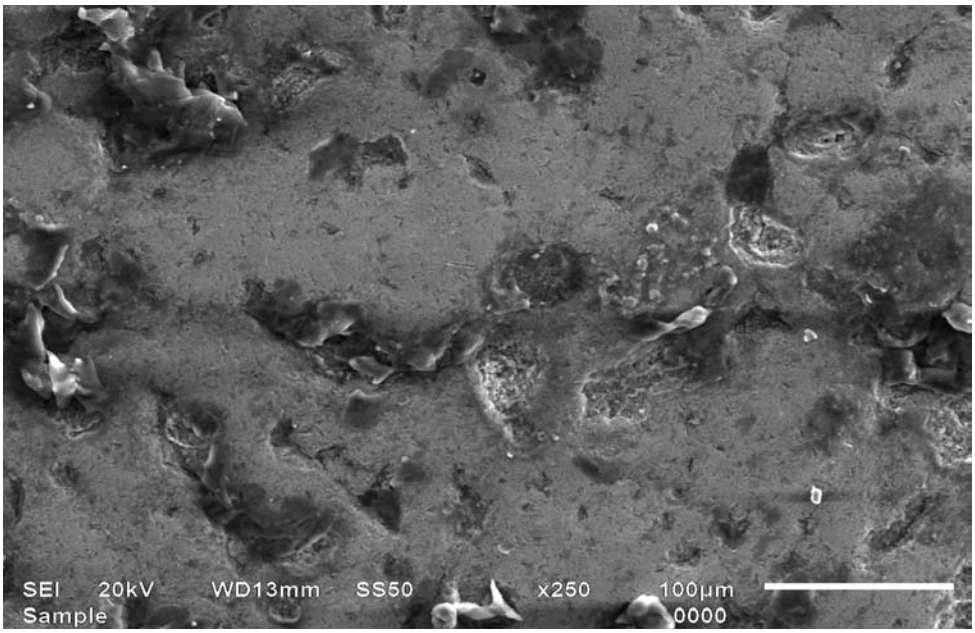

Fig. 6.9 SEM image of uncoated grey cast iron specimen before wear at impact angle of 30° and flow velocity of 69.8 m/sec at 250X magnification

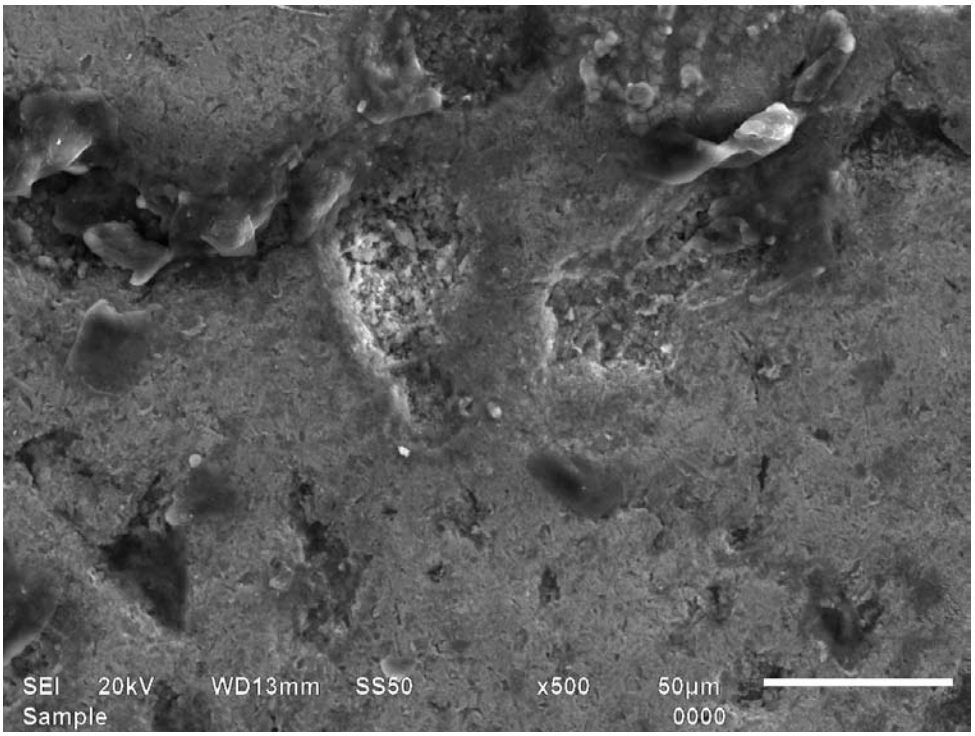

Fig. 6.10 SEM image of uncoated grey cast iron specimen after wear at impact angle of 30° and flow velocity of 69.8 m/sec at 500X magnification

The SEM results shows that the erosion wear is mainly due to scratching or cutting mechanism for both coated and uncoated samples and Ni coated specimen shows a smoother surface and hence has high resistance to erosion wear due to high hardness as compared to that of uncoated specimen.

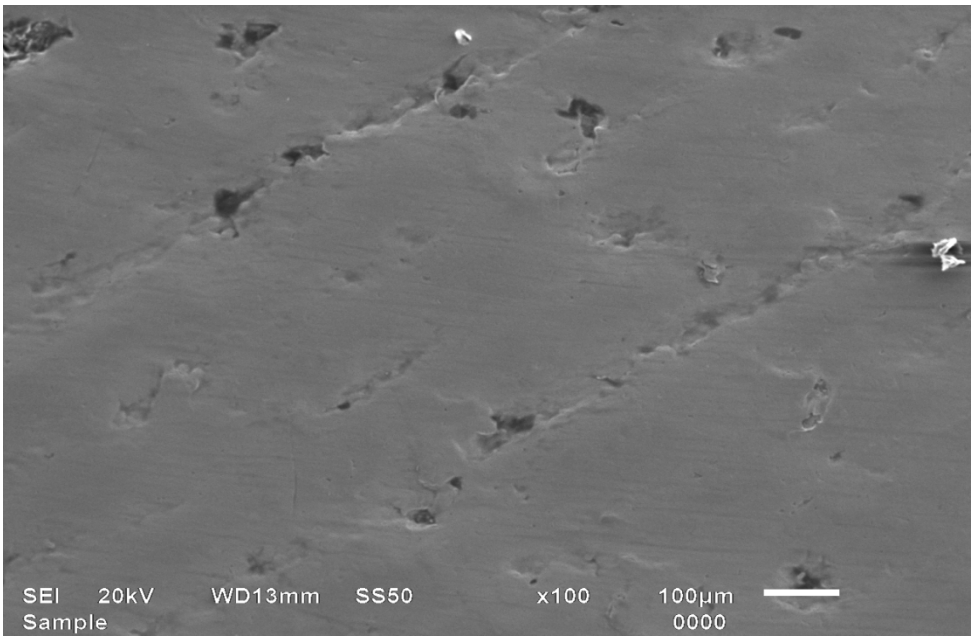

Figure 6.11 SEM image of Ni coated grey cast iron specimen before wear at impact angle of 30° and flow velocity of 69.8 m/sec at 100X magnification

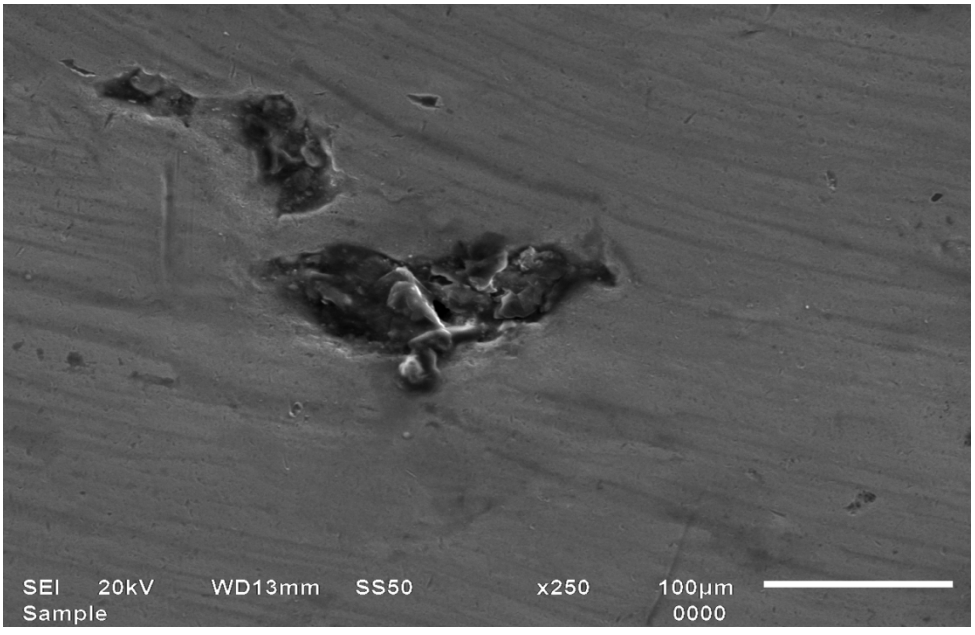

Figure 6.12 SEM image of Ni coated grey cast iron specimen after wear at impact angle of 30° and flow velocity of 69.8 m/sec at 250X magnification

CHAPTER 7

CONCLUSION AND FUTURE SCOPE

CONCLUSION

Erosion wear is a serious problem that constantly accompanies the operation of the system for hydraulic transportation of solid materials. The consequences are the loss of material (steel); loss of work element's working capacity, great operational expenses, etc. The choice of new materials for working elements, improvements in construction, and optimization of the slurry flow are all various ways of softening the consequences of erosion wear that reflects on the working life of the hydraulic transportation pump's elements. The grey cast iron selected as a base material of pumping system. The electroplating technique is used for coating of nickel hard on base material. It is observed that the erosion wear of both coated and uncoated specimens shows inverse proportionality with impact angles being highest at 30º and lowest at 90º.Also the SEM images shows that the wear is mainly due to the scratching phenomenon due to brittle nature of grey cast iron specimens. The erosion wear increases with increase in flow velocities as at high velocities high kinetic energy is available at the surface of the specimen which causes more erosion wear to take place.

The erosion pot tester is designed for study of the erosion wear behavior of slurry transportation systems with high concentration.

FUTURE SCOPE

- The erosion wear studies can be performed with other coating techniques.
- The computational approach can be used to simulate the similar work with different operating conditions.
- The effect of erosion wear of pump impeller of ash disposal system can be studied.
- The similar erosion wear studies can be extended by using other types of pot tester and different slurry concentration.

REFERENCES

1. Ahmed Elkholy,"Prediction of abrasion wear slurry pump materials", Wear 84(1983) 39-49.

2. M A Rayan, M Shawky, "Evaluation of wear in a centrifugal pump", Proc Instn Mech engrs(1989) Vol 203.

3. Gupta, R., Singh, S. N. and Seshadri, V. (1995), "Prediction of uneven wear in a slurry pipeline on the basis of measurements in a pot tester", Wear, 184, 169-178.

4. Clark, H. M. and Wong, K. K. (1995), "Impact angle, particle energy and mass loss in erosion by dilute slurries", Wear, 186-187, 454-464.

5. Mishra, R., Singh, S. N., and Seshadri, V., (1998), "Study of characteristics and solid distribution in constant area and erosion-resistant long-radius pipe bends for the flow of multisized particulate slurries", Wear, 217, 297-306.

6. Gandhi BK, V. Seshadri, "Study of parametric dependence of erosion wear for the parallel flow of solid- liquid mixtures", Tribology international 32(1999) 275-282.

7. Stack, M. M., and Pungwiwat, N., (1999), "Slurry erosion of metallics, polymers, and ceramics: particle size effects", Materials Science and Technology, 15, 337-344.

8. Sellgren, A., Addie, Graeme and Scott, Stephen, (2000), "The effect of sand-clay slurries on the performance of centrifugal pumps." The Canadian J. Chemical Engg., vol.78 USA, pp. 764-769.

9. Craig I. Walker, Greg C. Bodkin, "Empirical wear relationships for centrifugal slurry pumps" Part 1: side-liners, Wear 242(2000) 140-146.

10. Gandhi BK, Singh S.N, Seshadri V, "Variation of Wear along the Volute Casing of a Centrfugal Slurry Pump", JSME international Journal(2001) Vol. 44, No. 2.

11. Craig I. Walker, "Slurry pump side- liner wear: comparison of some laboratory and field results", Wear 250 (2001) 81-87.

12. O'Flynn, D. J., Bingley, M. S., Bradley, M. S. A., and Burnett, A. J., (2001), "A model to predict the solid particle erosion rate of metals and its assessment using heat-treated steels", Wear, 248, 162-177.

13. S.N. Singh, Gandhi BK, “Study on the effect of surface orientation on erosion wear of flat specimens moving in a solid-liquid suspension”, Wear 254(2003) 1233-1238.

14. R.J. Llewellyn, S.K. Yick , K.F. Dolman, “Scouring erosion resistance of metallic materials used in slurry pump service”, Wear 256 (2004) 592–599.

15. Satish V. Borse , Gandhi BK, “Nominal particle size of multi-sized particulate slurries for evaluation of erosion wear and effect of fine particles”, Wear 257(2004) 73-79.

16. Aubin, J., Sauze, N. Le, Bertrand, J., Fletcher, D. F., and Xuereb, C., (2004), “PIV measurements of flow in an aerated tank stirred by a down- and an uppumping axial flow impeller”, Experimental Thermal and Fluid Science, 28, 447-456.

17. Girish R. Desale, Bhupendra K. Gandhi ∗, S.C. Jain, “Improvement in the design of a pot tester to simulate erosion wear due to solid–liquid mixture”, Wear 259 (2005) 196–202.

18. Das, Y.L. Saraswathi, D.P. Mondal, “Erosive–corrosive wear of aluminum alloy composites: Influence of slurry composition and speed”, Wear 261 (2006) 180–190

19. G.R Desale , B.K Gandhi , S.C Jain, “Effect of erodent properties on erosion wear of ductile type materials”, Wear 261(2006) 914-921.

20. T. Manisekaran, M. Kamaraj, S.M. Sharrif, and S.V. Joshi, “Slurry Erosion Studies on Surface Modified 13Cr-4Ni Steels”: Effect of Angle of Impingement and Particle Size ASM International (2006) 1059-9495.

21. M. C. Lin, L.S. Chang, H.C. Lin, C.H. Yang, K. M. Lin, “ A study of high speed slurry erosion of NiCrBSi thermal sprayed coating”, surface and coatings technology 201 (2006) 3193/3198.

22. M.A. Al-Bukhaiti , S.M. Ahmed, F.M.F. Badran , K.M. Emara, “Effect of impingement angle on slurry erosion behaviour and mechanisms of 1017 steel and high-chromium white cast iron”, Wear 262 (2007) 1187–1198.

23. M.N. Noui-Mehidi ∗, L.J.W. Graham, J. Wu, B.V. Nguyen, S. Smith, “Study of erosion behaviour of paint layers for multilayer paint technique applications in slurry erosion”, Wear 264 (2008) 737–743.

24. Feng Jianjun, Karl Friedrich, and Dohmen Hans Josef, (2007), “Numerical investigation on pressure fluctuations for different configurations of vaned diffuser pumps”, International Journal of Rotating Machinery ,Vol 2007, Article ID 34752.

25. Y. A. Khalid and S.M. Sapuan, “Wear analysis of centrifugal slurry pump impellers”, Industrial Lubrication and Tribology 59/1 (2007) 18-28.

26. Cheah K.W, Lee T. S. ,Winoto S. H., and Zhao Z.M. ,(2007), “Numerical flow simulation in a centrifugal pump at design and off-design conditions”, International Journal of Rotating Machinery,Vol (2007), Article ID 83641.

27. Roudnev A, Kosmicki R 2007, “Effects of CFD modelling configuration on centrifugal slurry pump casing wear prediction”, The 17th International Conference on the Hydraulic Transport of Solids.

28. Desale GR, Gandhi BK, Jain SC, “Slurry erosion of ductile materials under normal impact condition” Wear 264(2008) 322-330.

29. Jain SC, Gandhi BK, Desale GR, (AA 6063), “Particle size effects on the slurry erosion of aluminium alloy”, Wear 266 (2009) 1066-1071

30. Zhou Guanghong,Ding Hongyan, ZhangYue,LiNianlian, “Corrosion–erosion wear behaviours of 13Cr24Mn0.44N stainless steel in saline–sand slurry”. Tribology International 43 (2009) 891–896.

31. R.C. Shivammurthy, M. Kamraj, R. Nagrajan, S.M. Shariff, and G. Padmanabham, “Slurry Erosion Characteristics and Erosive Wear Mechanisms of Co-Based and Ni-Based Coatings Formed by Laser Surface Alloying”, The Minerals, Metals & Materials Society and ASM International 2009

32. Kalekudithi ekambara, R. Sean Sanders, “Hydraulic simulation of horizontal slurry pipeline using ansys CFX”, Journal of American Chemical Society, Vol XXX, 2009.

33. L.J.W. Graham, D. Lester and J. Wu, “Slurry Erosion in Complex flows:experiment and CFD”**,** Seventh International Conference on CFD in the Minerals and Process Industries,CSIRO, Melbourne, Australia,9-11 December 2009

34. S. Haavisto, J. Syrjanen, A. Koponen, M. Manninen (2009)," Particle velocity and concentration profiles of sand-water slurry in stirred tank-measurement and modelling ". Seventh Inernational conference on CFD in the Minerals and Processing Industries, CSIRO, Melbourne, 9-11 December.

35. S.L. Liu∗, X.P. Zheng, G.Q. Geng, **"**Influence of nano-WC–12Co powder addition in WC–10Co–4Cr AC-HVAF sprayed coatings on wear and erosion behavior", Elsevier,Wear 269 (2010) 362–367.

36. Cunkui Huanga, P. Minevb, Jingli Luoc, K. Nandakumard, "A phenomenological model for erosion of material in a horizontal slurry pipeline flow", Wear 269 (2010) 190–196

ANNEXURE I

S.No	SIZE RANGE(IN MICRONS)below	% Finer Bottom	Xi bottom	Wi bottom	wixi bottom	Dwmi bottom
1	2000	100%	600	26.26	15756	
2	1400	89.40%	690	10	6900	
3	710	85.52%	355	32.23	11441.65	
4	355	72.61%	55	19.5	1072.5	
5	300	65%	50	15.51	775.5	
6	250	58.90%	38	30.2	1147.6	**161.8695**
7	212	46.80%	32	6.78	216.96	
8	180	44.14%	30	58.73	1761.9	
9	150	20.65%	25	8	200	
11	125	17.41%	35	9.78	342.3	
12	90	13.48%	15	26.25	393.75	
13	75	4%	75	7.31	548.25	

Table 1.1 Particle size distribution of bottom ash

ANNEXURE II

time(min)	cw10 % (bottom ash)	cw20 % (bottom ash)
0.17	24.622	20.5
0.33	30.662	23.25
0.50	32.665	25.65
0.67	33.768	25.85
0.83	34.348	26.32
1.00	36.213	26.5
1.17	40.627	28.12
2	41.47	31.16
3	41.47	38.37
4	41.47	42.25
5	41.47	44.39
15	41.47	44.39
30	41.47	44.39
60	41.816	45.54
120	41.992	45.54
180	43.348	45.54
240	43.348	46.01
480	43.709	46.01

Table 1.2 Settling Characteristics of bottom ash slurry

ANNEXURE III

Concentration →	10%	20%	30%	40%	50%
Shear Stress, Shear Rate ↓					
0	0	0	0	0	0
50	0.05	0.075	0.11	0.195	0.44
75	0.08	0.1425	0.165	0.2925	0.58
100	0.11	0.15	0.28	0.39	0.63
125	0.13	0.1975	0.29	0.5275	0.79
150	0.15	0.225	0.39	0.6	0.84
175	0.18	0.2625	0.39	0.7	0.98
200	0.24	0.34	0.48	0.83	1.32
225	0.28	0.37	0.61	0.98	1.46

Table 1.3 Shear Stress- Shear rate of bottom Ash slurry at different concentrations

Concentration (Cw) %	Relative viscosity
0	1
10	1.02
20	1.61
30	2.21
40	4.32
50	5.62

Table 1.4 Concentration Vs relative viscosity of bottom ash slurry

Concentration (Cw)%	pH
0	7.75
20	7.67
25	7.66
30	7.66
35	7.64
40	7.63
45	7.62
50	7.62

Table 1.5 Concentration Vs pH value of bottom ash slurry

ANNEXURE IV

Cummlative Weight loss (mg) / Time (hours)	At impact angle 30º		At impact angle 60º		At impact angle 90º	
	uncoated	Ni- coated	uncoated	Ni- coated	uncoated	Ni- coated
1	42	27	29	17	24	8
2	73	38	62	38	43	24
3	116	68	97	53	61	38
4	155	86	121	69	83	47

Table 1.6 Variation of cummlative weight loss v/s time at 34.8 m/sec velocity of flow

Cummlative Weight loss (mg) / Time (hours)	At impact angle 30º		At impact angle 60º		At impact angle 90º	
	uncoated	Ni- coated	uncoated	Ni- coated	uncoated	Ni- coated
1	51	39	35	13	29	10
2	93	48	78	37	55	28
3	142	79	118	55	82	51
4	192	94	154	81	114	65

Table 1.7 Variation of cummlative weight loss v/s time at 51.8 m/sec velocity of flow

Cummlative Weight loss (mg) / Time (hours)	At impact angle 30º		At impact angle 60º		At impact angle 90º	
	uncoated	Ni- coated	uncoated	Ni- coated	uncoated	Ni- coated
1	57	31	42	28	33	19
2	105	63	86	51	70	36
3	160	88	134	78	102	58
4	211	127	176	83	137	74

Table 1.8 Variation of cummlative weight loss v/s time at 69.7 m/sec velocity of flow